

West Valley High Time Resolution Air Toxics Monitoring Campaign Report

**Submitted to the United States Environmental Protection Agency and
Utah Division of Air Quality (UDAQ)**

November 28, 2017

Project Manager

Patrick Barickman, Utah Division of Air Quality, Salt Lake City, UT

Principal Investigators

Dr. Munkhbayar Baasandorj, Atmospheric Sciences, University of Utah, Salt Lake City, UT

Dr. Jaron Hansen, Brigham Young University, Provo, UT

Investigators

Roman Kuprov, Utah Division of Air Quality, Salt Lake City, UT

Dr. Delbert Eatough, Brigham Young University, Provo, UT

Dr. Paul Cropper, Brigham Young University, Provo, UT

Devon Orsen, Brigham Young University, Provo, UT

Dr. John Lin, Atmospheric Sciences, University of Utah, Salt Lake City, UT

Dr. Dylan Millet, University of Minnesota, St. Paul, MN



TABLE OF CONTENTS

1. ACKNOWLEDGEMENTS	3
2. EXECUTIVE SUMMARY	4
3. INTRODUCTION	6
4. METHODS.....	7
4.1. Site Description	8
4.2. Particulate Measurements	9
4.3. Trace Gas Measurements.....	11
4.4. Positive Matrix Factorization (PMF) Analysis for Source apportionment.....	13
4.5. STILT Back Trajectory Analysis.....	14
4.6. Site Comparison	14
5. RESULTS AND DISCUSSION.....	14
5.1. Overview.....	14
5.1.1. Winter Campaign.....	14
5.1.2. Summer Campaign.....	19
5.2. Source Apportionment Analyses	21
5.2.1. Temporal and spatial variability	21
5.2.2. PMF analysis for Source Apportionment.....	31
5.2.3. Back-trajectory analysis.....	43
6. IMPLICATIONS FOR AIR QUALITY	47
7. PUBLIC OUTREACH.....	50
8. SUMMARY.....	51
9. REFERENCES	53

1. Acknowledgements

We would like to acknowledge the US Environmental Protection Agency for funding this study. The authors would like to acknowledge Dr. Dylan Millet from University of Minnesota, St. Paul, MN for deploying the PTR-MS instrument, Dr. John Lin from University of Utah for STILT modeling, Utah DAQ's AMC group, in particular Mark Squire, Ken Simons and Phil Harrison for their help during the campaign and Chris Pennell from UDAQ's Technical Analysis team for his collaboration, Neil Armstrong Academy for hosting the site, and Dr. John Horel and his team at University of Utah for MESOWEST surface meteorological observations.

2. Executive Summary

Majority of Utah's population live along the Wasatch Mountains in Northern Utah. Like many urban mountain valleys in the Intermountain West, the Utah valleys experience periods of atmospheric stable conditions with elevated fine particulate matter (particulate matter with aerodynamic diameter less than 2.5 micron, PM_{2.5}) and other primary pollutants in winter. In contrast, high ozone is common in summer due to the high temperatures and high elevation with strong sunlight. Hence, there is a need to study the hazardous air pollutants (HAPs) in different seasons. HAPs are those pollutants known or suspected to cause cancer and other serious health effects. Ambient HAPs have been monitored in the Salt Lake Valley since 2002. The past studies of HAP's in the SLV were useful in determining their seasonal trends, but they lacked time resolution to enable source apportionment analysis. The West Valley High Time Resolution Air Toxics Monitoring Campaign was conducted to fill this gap and determine the ambient levels of HAPs in December – February, a peak season for PM_{2.5} pollution, and in June – August, a peak season for photochemistry, and characterize their sources in Utah's Salt Lake Valley.

As part of West Valley High Time Resolution Air Toxics Monitoring campaign, a wide array of gaseous and particulate HAPs and related species were monitored at Neil Armstrong Academy located in the West Valley City to provide real-time observations of trace gas and particulate composition during summer and winter season. Key analyzers at this site were high-sensitivity Proton Transfer Reaction-Mass Spectrometer (PTR-MS) and Organic Aerosol Monitor that enabled the first simultaneous, co-located direct measurements of volatile organic compounds and particle bound organic species in the SLV. Our observations indicate higher levels of the pollutants including PM_{2.5} and monitored HAPs in winter compared to those in summer months due to the shallow boundary layer and the episodic stagnant conditions. Three different analyses a) temporal and spatial trends analysis, b) Positive Matrix Factorization (PMF) analysis and c) 24-hour back trajectory analysis were conducted for better source apportionment of HAPs and related species. High time resolution observations of VOCs indicate a wide variety of OVOC sources including mobile, point (solvent use, paint stripping etc.) and secondary sources. Temporal and spatial trends of HAP's and their relationship with marker species were carefully examined for source identification. Among the suite of HAPs monitored, the light aldehydes such as HCHO and CH₃CHO are observed at high levels, showing sporadic, instantaneous enhancements during the week, frequently at night. The average wind pattern and 24-hour back trajectory analysis indicate aldehyde sources located to the south and provide a consistent footprint of a source region that encompasses a narrow trajectory in the southern part of the SLV along the urban corridor and a wider footprint in Utah Valley.

The observed and predicted PM_{2.5} composition by PMF analysis consistently suggest that the total PM_{2.5} mass is dominated by secondary species that accounts for ~ 70 % of total during the periods with elevated PM_{2.5}. The PMF analysis of 689 hourly averaged data sets identified a diesel emissions related factor that contained 41% of the NO_x and 84% of the BC. This factor is present at relatively low levels with an average concentration of 0.6 µg/m³, thus its contribution to the total mass is found to be minor in winter. This finding is not surprising considering the fact that the distance to the nearest highway is

~2 - 3 miles. However, this finding does not eliminate a potential significance of DPM as a HAP in the residential areas in close proximity to the major highways in the SLV.

One of the major outcomes of this work worth emphasizing is the air quality implications. A rich dataset of gaseous and particulate species collected as part of West Valley High Time Resolution Air Toxics Monitoring campaign was used for a comprehensive analysis that shed light on the fundamental chemical and meteorological processes underlying adverse air quality in the SLV in winter and motivated further in-depth research to help to reduce pollution and improve public health and welfare.

3. Introduction

Utah has been one of the fastest growing states in the nation for the past six years. In 2010, ~ 80% of Utahns live in urban areas along the Wasatch Front and the population growth is projected to continue in existing urban areas². The densely populated Salt Lake Valley is surrounded by the Wasatch Mountains to the east and the Oquirrh mountains to the west, and is open to the Great Salt Lake to the northwest. The unique topography and meteorological conditions of the Salt Lake Valley (SLV) favor air stagnation that traps air pollutants for several consecutive days in winter, leading to high pollutant levels³⁻⁶. During these events, atmospheric pollutants such as NO_x, CO and particulate matter with aerodynamic diameter less than 2.5 micron (PM_{2.5}) are found to accumulate in the valley, with PM_{2.5} levels exceeding the National Ambient Air Quality Standard (NAAQS) for PM_{2.5} about 18 times per year^{1, 5}. The adverse health effects of these episodes are seen in increase in emergency room admissions due to respiratory symptoms such as aggravation of asthma and pneumonia⁷. The Wasatch Front also experiences high levels of ozone (O₃) occasionally exceeding the NAAQS for ozone on clear summer days with high temperature and strong solar insolation⁸⁻⁹. During these periods, photochemical production of secondary species such as carbonyls and aldehydes becomes important.

HAPs, also known as air toxics, are those pollutants that are known or suspected to cause cancer and other serious health effects, such as reproductive effects or birth defects, or adverse environmental effects. Under the Clean Air Act, EPA is required to regulate emissions of HAPs. The current list includes 187 HAPs that include BTEX compounds (otherwise known as benzene, toluene, ethylbenzene and xylenes), chlorinated species such as perchloroethylene and methylene chloride, persistent organic pollutants (POPs) such as dioxin and PCBs, and metals such as mercury and lead¹⁰. Like all primary pollutants, ambient hazardous air pollutants (HAPs) are expected to be enhanced under the stagnant conditions in winter, hence there is a need to identify the most important HAP's in the Salt Lake Valley and to determine their levels and sources. Ambient HAPs have been monitored at the Bountiful monitoring station since 2002 as part of the National Air Toxics Trends Stations (NATTS) program. Analyses of 2002 – 2013 data indicated a set of eleven gaseous organic HAPs that might be of importance in the Salt Lake Valley including 1,3-butadiene; 1,4-dichlorobenzene; acetaldehyde; acrylonitrile; benzene; carbon tetrachloride; dichloromethane; ethylbenzene; ethylene dichloride; formaldehyde; and tetrachloroethylene. Following this analysis, Utah Division of Air Quality conducted year-long air toxics study in 2015-2016 in order to characterize the spatial distribution and seasonal trends of HAPs and collected gaseous volatile organic compounds (VOCs) and toxic metals in PM₁₀ samples in West Valley City, Bountiful (current NATTS site), and Lindon in the Utah Valley one-in-three days¹¹. This study found high levels of formaldehyde, acetaldehyde and methylenechloride at the Bountiful site. Kuprov¹¹ noted the uncommon seasonal trends of formaldehyde and acetaldehyde that showed wintertime maximum and attributed it to the sources in that area including the local refineries, painting or paint stripping operations, and others. West Valley high time resolution air toxics monitoring campaign aimed to improve upon the temporal resolution of previous studies and provide real-time data.

Technical Objectives of this study are to:

- 1) *determine the ambient levels as well as the spatiotemporal variation of HAPs in the Salt Lake and Utah Valleys, including gas phase carbonyls (formaldehyde and acetaldehyde) and polycyclic aromatic hydrocarbons (PAHs) in both gas and particle phases;*
- 2) *determine the chemical speciation of PAHs and diesel particulate matter in the particle phase as well as estimate the particle toxicity during high PM_{2.5} pollution episodes in the winter and summer; and*
- 3) *conduct a source apportionment analysis using the high temporal resolution dataset of HAPs and related species.*

In order to achieve these goals, West Valley high time resolution air toxics monitoring campaign was conducted within the framework of community-scale Hazardous Air Pollutant (HAP) monitoring near a residential neighborhood in West Valley City, UT to complement the State's ongoing research on HAPs distribution across the Salt Lake urban area. As part of this study, two intensive campaigns were conducted in West Valley City during winter (December 2015 - February 2016) and summer (June - August 2015) and generated a comprehensive, temporally resolved dataset of hazardous air pollutants (HAPs) in the gas and particulate phases and species related to emissions of HAPs. The methods section describes the details of the measurements and analysis methods. Results and discussion section provide 1) an overview of the winter and summer campaigns and 2) the details of data analyses. Three different analyses, including temporal and spatial trends analysis, Positive Matrix Factorization (PMF) analysis and 24-hour back trajectory analysis were conducted for better source apportionment of HAPs and related species as described in Section 5. A Positive Matrix Factorization (PMF) analysis was conducted to identify probable sources of the fine particulate material. Input to the analysis included the FDMS TEOM measured fine particulate mass, the major chemical components of PM_{2.5} (NVOM, SVOM, BC, ammonium nitrate, ammonium sulfate, chloride and sodium), gas phase species which contribute the identification of sources and secondary chemistry (CO, NO_x and NO₂) and specific markers of primary and secondary contributors to PM_{2.5} (Fluorene, Levoglucosan, Dehydroabietic Acid, Syringe Aldehyde, o-Phthalic Acid, Adipic Acid, 4-oxyheptanedioic Acid, Methanol and C8 Aromatics). A total of 689 hourly averaged data sets were available for this analysis. Temporal and spatial variability of gaseous HAP's including BTEX compounds, carbonyls, and aldehydes were examined to characterize their levels and sources. 24-hour back trajectory analysis was conducted using Lagrangian STILT model to obtain footprints associated with periods with high levels of HAPs. The implications of these findings on the air quality in the SLV are discussed in Section 6. The following sections 7 and 8 provide a description of the public outreach component and a summary of the study.

4. Methods

Two intensive campaigns were conducted in West Valley City during winter (December 2015 - February 2016) and summer (June - August 2015). As part of this study, a wide suite of trace gas and particulate measurements were made at this location to monitor continuously the ambient HAPs and their tracers,

and examine their sources. Table 1 shows the instrumentation at NAA. Meteorological data was obtained from the MesoWest network¹².

4.1. Site Description

The measurement site is located at the Neil Armstrong Academy (NAA) situated on the valley floor of the Salt Lake Valley as shown in Figure 1. This site was chosen because of its central location and low elevation, which makes it susceptible to a buildup of high levels of PM_{2.5} and other pollutants during winter months. There are the several major highways running on its eastern and northern borders. The eastern part of the town is below the landing approach paths for the Salt Lake City International Airport. The local industries and refineries are located at the northern edge of the city, northeast from the site.

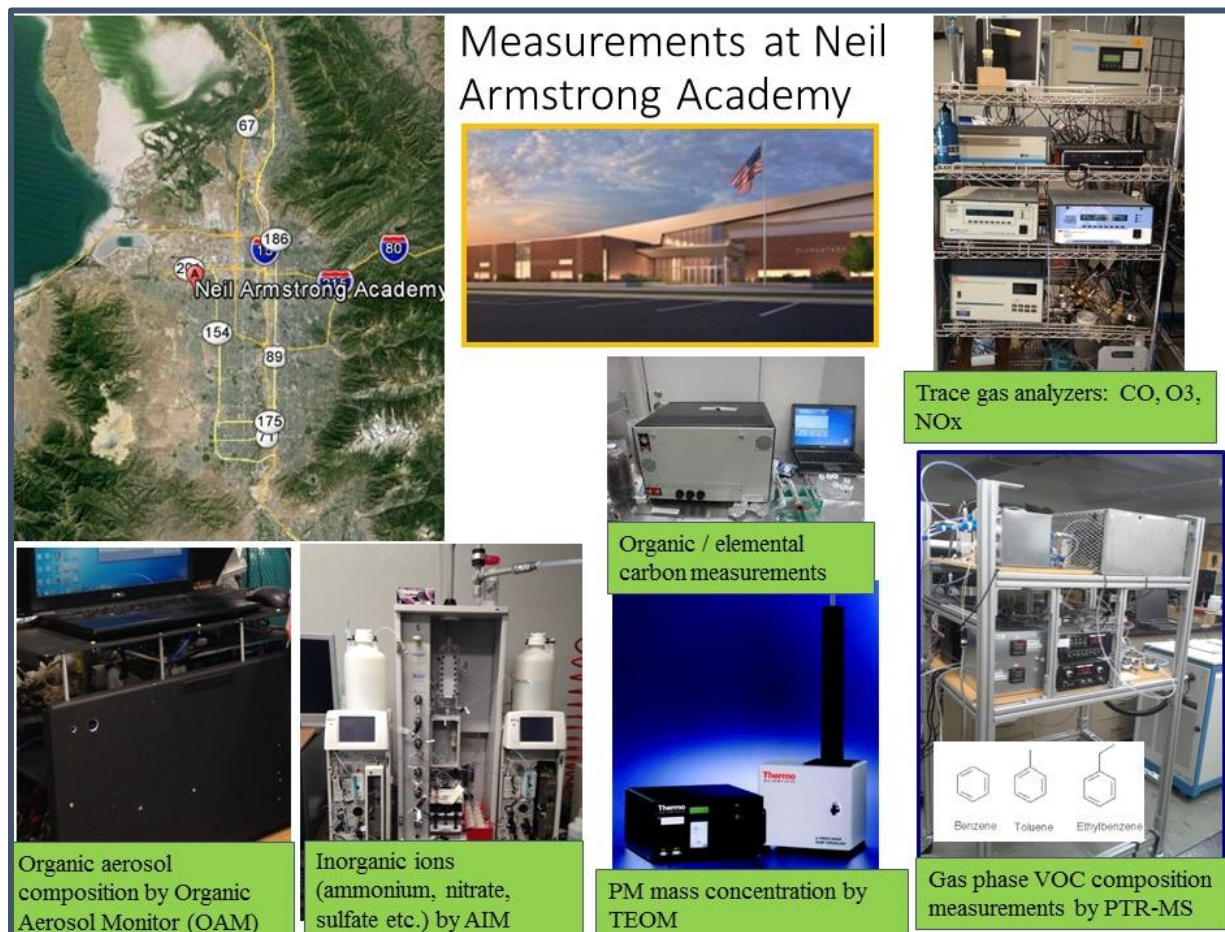
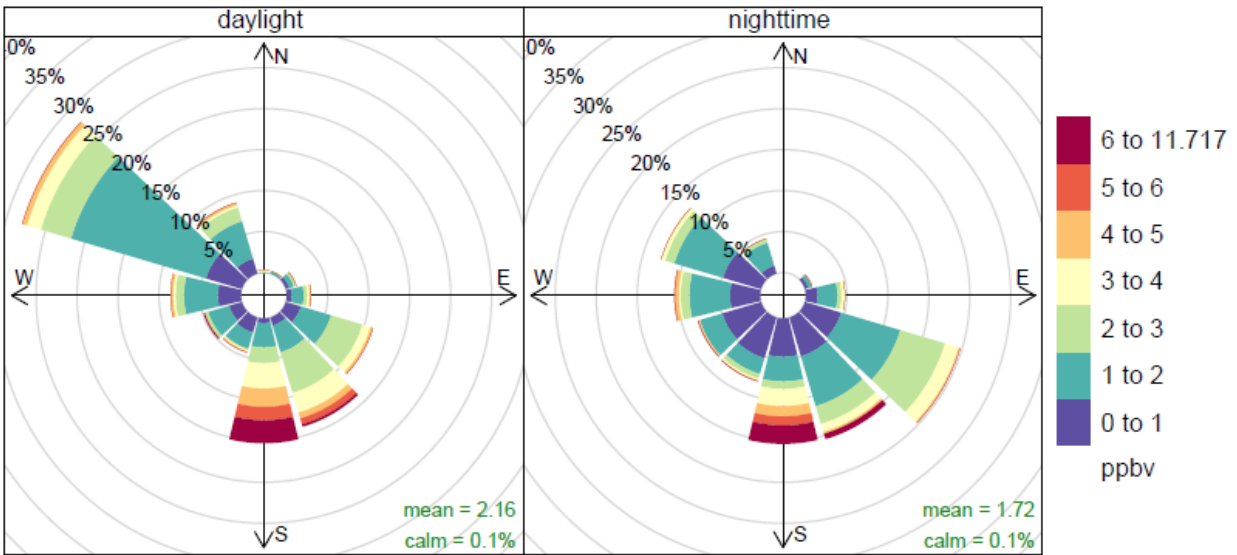


Figure 1 shows the location of the measurement site at Neil Armstrong Academy (NAA) in West Valley City, UT. The pictures show the instruments deployed at NAA to measure gaseous and particulate HAPs in real-time.

wind spd.



Frequency of counts by wind direction (%)

Figure 2: Windrose at NAA indicating predominant winds are northwesterly during the day and southeasterly at night

The wind rose in Figure 2 indicate that the predominant winds are northwesterly during the day and southeasterly at night. Hence, the site is often impacted by lake-breeze during the day and southerly flows at night. Influence from northeast appears to be minor indicating the site is impacted by the emissions from refineries to lesser extent. However, the site is frequently influenced by the easterly and southeasterly flows, which transport pollutants from the urban corridor of Salt Lake Valley.

4.2. Particulate Measurements

PM_{2.5} mass concentrations were measured using an R&P Model 8599 FDMS (Filter Dynamics Measurement System) Tapered Element Oscillating Microbalance (TEOM) 1400ab sampler. The FDMS TEOM measures all fine particulate mass including ammoniums nitrate and semi-volatile organic material but does not measure fine particulate water. Black carbon (BC) and UV absorbing carbon were determined with a dual wavelength Aethalometer (Magee Scientific). Aerosol carbon was measured with a Sunset Lab instrument, providing elemental carbon (EC) and nonvolatile organic carbon (NVOC). The NVOC values were converted to nonvolatile organic mass, NVOM, using a factor of 1.6. Semi-volatile organic mass (SVOM) was estimated as the FDMS TEOM measured PM_{2.5} minus the sum of the fine particulate ionic and carbonaceous components described below.

Table 1 List of target HAPs and related species measured during this campaign

Species			Instrument	Resolution	Institution
Gas Phase					
VOCs	PAH	Benzene, C8 aromatics (sum of xylenes and ethylbenzene), C9 aromatics (sum of trimethylbenzenes, propyl benzenes and ethyltoluenes)	PTR - MS	~ 2 -3 min	UoU/UMN
	Carbonyl	Acetaldehyde, formaldehyde, C3-C6 ketones			
	Others	Acetonitrile, methanol, Carboxylic acids, isoprene			
Others		CO, Ozone, NO _x , NO ₂	Various	~ min	UDAQ
Particulate Phase					
Organic compounds	PAHs, Others	Levoglucosan, stearic acid, dehydroabiatic acid, pyrene, fluorine, galactosan, mannosan, phenanthrene, benzo (b and k) fluoranthene, o-phthalic acid, palmitic acid, vanillic acid, syringic acid, 4-oxoheptanedioic acid, retene, syringe aldehyde, 4-hydroxobenzoic acid, adipic acid, 4-aminobenzoic acid, 3-methyl-4-nitrophenol, 2,4,6-trimethylphenol, 1,3,5-triphenolbenzene, cis-pinonic acid, cholesterol, pentacecane, diazon, 9-anthracenecarboxaldehyde, 9-phenanthrenecarboxaldehyde, coronene	OAM	hourly	BYU

Black carbon (BC)			Aethalometer, Sunset Carbon Monitor	hourly	
Inorganics	Anions	Nitrate, sulfate, chloride	URG AIM monitor	hourly	UDAQ
	Cations	Ammonium, Sodium, Calcium, Potassium, and Magnesium			
Total PM _{2.5} mass			FDMS TEOM	hourly	UDAQ
Meteorological Parameters by University of Utah					

Fine particulate inorganic ionic composition was monitored using a URG 9000D AIM¹³. URG-9000 collected ambient particulate and gaseous samples on hourly basis. The sample data was separated into cations and anions for both phases as shown in Table 2. The ions that were below detection limit were omitted from the analysis as indicated by the crossed out cells.

Table 2 gives the gas and particle phase anions and cations measured by URG 9000.

Species								
Particles	Anion	Fluoride	Chloride	Nitrite	Bromide	Nitrate	Sulfate	Phosphate
	Cation	Sodium	Ammonium	Potassium	Calcium			
Gases	Anion	Fluoride	Chloride	Nitrite	Bromide	Nitrate	Sulfate	Phosphate
	Cation	Sodium	Ammonium	Potassium	Calcium			

The fine particulate organic composition and speciation was determined using GC/MS Organic Aerosol Monitor (GC-MS OAM)¹⁴⁻¹⁵. The instrument combines fully automated filter collection of fine particles with thermal desorption, gas chromatography and mass spectrometry to quantitatively measure the carbonaceous components of PM on an hourly averaged basis. It uses a chemically deactivated quartz filter for collection followed by thermal desorption and GC-MS analysis. Compounds measured by the GC-MS OAM and used in the PMF analysis included Fluorene, Levoglucosan, Dehydroabiatic Acid, Syringe Aldehyde, o-Phthalic Acid, Adipic Acid and 4-Oxoheptanedioic Acid (Table 1).

4.3. Trace Gas Measurements

CO, O₃ and NO_x (NO, NO₂) were monitored using analyzers from UDAQ, which included Teledyne Advanced Pollution Instrumentation (API) gas filter correlation CO analyzer (Model 300 E), photometric ozone analyzer (Model 400 E), and T series NO_x analyzer (Model T200U) equipped with NO₂ photolytic converter, respectively. The trace gas analyzers were calibrated bi-weekly and daily automated

precision, zero and span (PZS) checks are performed automatically to monitor any drifts. The ambient air was drawn into the room at ~ 10 LPM through ~ 10 m long ½" O.D. PFA tubing to a 6-port glass manifold. The trace gas analyzers sub-sampled from this manifold at 600 – 700 sccm.

A wide suite of volatile organic compounds (VOCs) was measured using a high sensitivity standard Proton Transfer Reaction - Mass Spectrometry (PTR-MS) that was brought from the University of Minnesota. Details about the instrumentation including the gas sampling inlet system for the PTR-MS instrument have been discussed previously (Figure 1)¹⁶⁻¹⁸. The ambient air was drawn in through ~ 8 m long ½" O.D. heated inlet at ~ 10 LPM and the inlet system sub-sampled 700 standard cubic centimeters per minute (sccm) of the total flow and the PTR-MS instrument sampled at ~ 35 sccm. The PTR-MS drift tube pressure and voltage were maintained at 2.3 mbar and 600 V ($E/N = 126$ Td), with the water flow at 6.5 sccm. Automated background measurements were performed every two hours and calibrations were made every ~ 6 hours. Two calibration tanks containing several HAPs (Table 1) were used for automated calibration. The backgrounds and calibration factors were extrapolated for the ambient measurements and used to obtain the concentration in ppb¹⁹. The PTR-MS sensitivities for some VOCs show a humidity dependence and were corrected using reported correction factors when available¹⁹⁻²¹. Effects of the humidity on the measurement sensitivity can be seen in Figure 3, which shows an extreme example, where the sensitivity of HCHO is reduced by a factor of three under high RH conditions. The x-axis here is the ratio of $H_2O-H_3O^+$ to H_3O^+ , which can indicate changes in humidity. Even though HCHO calibration was performed automatically once in 6 hours, because of the low sensitivity of PTR-MS toward HCHO, its strong dependence on the ambient humidity and small drifts in the background, HCHO measurement had high uncertainty. Laboratory investigation of the humidity dependence of the sensitivity for HCHO showed more than a factor of three or four decrease as relative humidity increases (Figure 3). Because of the uncertainty associated with the HCHO measurement, we use the signal corresponding to HCHO (m/z 31) for spatial and temporal analysis to determine the trends and variability. The instrument's sensitivity toward CH_3CHO , on the hand, is ~ 17 ncps/ppb, higher than that of HCHO, which was on the range of 0.7 – 2 ncps/ppb, therefore PTR-MS measurement of CH_3CHO is robust with an estimated uncertainty of < 15%.

The PTR-MS measures all C8 and C9 aromatic compounds at m/z 107 and 121, respectively; here we use the approach of de Gouw et al.²¹ to calculate a weighted calibration factor for the sum of C8 aromatics based on the measured p-xylene sensitivity and its typical abundance relative to its isomers. Similarly, a weighted calibration factor for the sum of C9 aromatic compounds based on the measured 123-trimethylbenzene sensitivity was derived and used to calculate the concentration of the sum of C9 aromatic compounds. The measurement uncertainty for BTEX compounds calculated in this way is estimated to be < 20%²².

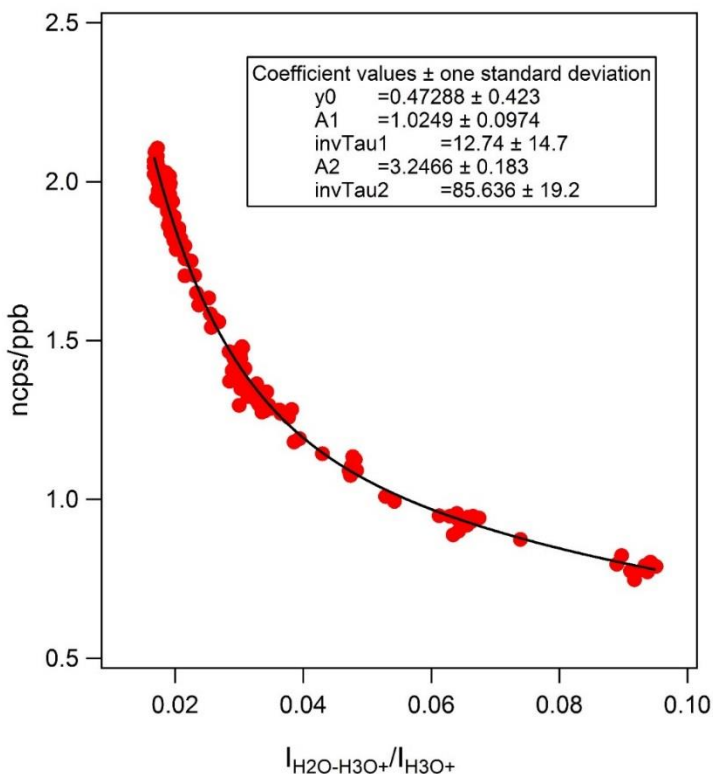


Figure 3: Humidity dependence of the PTR-MS response to HCHO at E/N 125 Td. A double exponential fit describes the humidity dependence of HCHO sensitivity and shows the large correction needed to predict the sensitivity as a function of relative humidity.

PTR-MS deployment allowed on-line detection of a broad range of HAPs including BTEX compounds and carbonyls (See Table 1) with high sensitivity and high-time resolution (~ 2 minutes).

4.4. Positive Matrix Factorization (PMF) Analysis for Source apportionment

689 data sets shown in Figures 18 - 20 were used for the PMF analysis. PMF2 and the algorithm used in the analysis has been previously described²³. With PMF2, the results are constrained so that factor contributions cannot be negative for any species. One of the advantages of PMF2 is the ability to account for missing and below detection limit data. The uncertainty in each measurement can be adjusted to account for aberrations in the data set. In this study, error uncertainty estimates were chosen similar to those previously outlined^{14,24}. For what were determined to be "reliable" data, the concentration values were directly used and the error estimates were assigned as the measurement error plus one third the limit of detection (LOD). In few instances when the measurement was below the LOD, the error was estimated as 5/6 the LOD. Missing values in the data set were accounted for by taking the geometric mean of the hour preceding and following the missing data point. In this study, SVOM concentrations were obtained as the difference between the FDMS TEOM and the sum of the other measured components of PM_{2.5}. Therefore, the error estimate was performed as mentioned above using the highest LOD of the various measurement techniques. The uncertainty of the fitted parameter, FDMS mass, was taken to be four times the measured value²⁵.

4.5. STILT Back Trajectory Analysis

Dr. John Lin (University of Utah, Dept. of Atmospheric Sciences) has provided detailed trajectory information for the NAA site during the 2015-2016 winter. These rely on hourly output from the High Resolution Rapid Refresh (HRRR) analysis fields provided by National Centers for Environmental Prediction (NCEP; 3km horizontal resolution), and the trajectory analysis within the STILT (Stochastic Time-Inverted Lagrangian Transport) model framework, as described in ²⁶⁻²⁷. The HRRR-STILT model carried out runs with 200 particles starting from the receptor, NAA, and transported backward in time for 24 hours. This analysis provided both trajectory and footprint source information for the events with high levels of oxygenated VOCs (OVOCs) including formaldehyde, acetaldehyde and acetone. The Backward in time trajectory analyses were also used in the interpretation of the PMF results.

4.6. Site Comparison

NO_x, O₃ and PM_{2.5} at NAA were compared with those at two other sites, Hawthorne (HW) and University of Utah (UU) in order to evaluate the spatial distribution of pollutants and gain insight into the variability in chemical composition within the SLV. HW is UDAQ's main air monitoring station for Salt Lake City located in the southeastern part of Salt Lake City. UDAQ monitors PM (PM_{2.5}, PM₁₀, PM_{10-2.5}), PM_{2.5} speciation, trace gases (O₃, NO_x, NO_y), and meteorological parameters at this site according to EPA guidelines²⁸. UU site is located at William Browning Building on the University of Utah campus, which is situated on the northeastern bench of the Salt Lake Valley, ~150 meters above the valley floor. This site is located away from major industrial areas and highways. A suite of trace gas and particulate measurements were conducted at UU during 2015-2016 winter as part the Salt Lake Valley Winter PM_{2.5} Study¹, which gave an opportunity to compare the levels of key atmospheric pollutants across the valley as discussed in the atmospheric implications section.

5. Results and Discussion

5.1. Overview

As part of this study, we conducted two field campaigns and obtained datasets consisting of gas and particulate species, and associated meteorology parameters in winter and summer months. The winter campaign (December - February) gave us an opportunity to sample 6 wintertime pollution episodes and examine the composition of particulate matter and the enhancements of HAPs during these episodes whereas the summer (June-August) study was focused more on the measurement of precursor gases, secondary sources for formaldehyde and acetaldehyde. Here we present a) an overview of winter and summer measurements b) the analysis conducted for better source characterization and c) implications for the air quality and public health.

5.1.1. Winter Campaign

Figure 4 gives an overview of the chemical observations made during the 2015-2016 winter. The SLV saw six multi-day pollution episodes with high PM_{2.5} that led to total of 9 exceedances during the 2015-2016 winter (Table 3). These episodes are closely related to the passing of high-pressure systems that lead to strong atmospheric stability or persistent cold air pools (PCAPs). Under these conditions, the boundary layer is stably stratified and/or capped by a capping inversion associated with warm air advection aloft^{1, 5-6}. During these events, atmospheric mixing is limited and pollutants emitted near the surface accumulate, often exceeding the National Ambient Air Quality Standard (NAAQS) for PM_{2.5}.

PM_{2.5} at NAA agreed well with observations from other sites in the valley as PM_{2.5} levels are relatively homogenous during these pollution episodes^{1,4}. NAA dataset along with measurements from Hawthorne and University of Utah site were used to investigate the chemical and meteorological processes driving these pollution episodes and details can be found in Baasandorj et al. ¹. Four of the pollution episodes of this season were short-lived episodes with moderate PM_{2.5} levels. 8 out of the 9 exceedances for PM_{2.5} occurred during a single pollution episode that took place between 6-16 February 2016 (Table 3). Concentrations of primary pollutants such as NO_x and CO were enhanced during the pollution episodes while O₃ levels are lower. However, the enhancements in VOC levels were not very obvious likely due to the slight enhancements in VOCs during pollution episodes that could be masked by the measurement uncertainty and interferences due to high RH conditions and fog events (see the method section). Nonetheless, the PTR-MS measurements showed sporadic enhancements in oxygenated VOCs (OVOCs), some of which are listed as HAPs. For example, CH₃CHO and CH₃OH levels as high as 70 and 250 ppb were observed during the study period (Figure 4). In contrast, other HAPs such as BTEX compounds and acetonitrile were detected at low or moderate levels. Section 5.2.1 explore this in detail.

Table 3: Summary of pollution episodes during 2015 -2016 winter season.

#	Start	End	# PM _{2.5} NAAQS exceedences
1	12/27/2015	12/31/2015	-
2	01/01/2016	01/07/2016	1 x (4 Jan. 2016)
3	01/12/2016	01/15/2016	-
4	01/22/2016	01/24/2016	-
5	01/27/2016	01/29/2016	-
6	02/06/2016	02/16/2016	8 x (7-14 Feb.2016)

The ionic composition measurements indicate that ammonium and nitrate ions are the most abundant ions with chloride, nitrite, sodium, and sulfate ions detected at low levels in most of the samples. The total PM_{2.5} measured by TEOM and sum of the fine particulate ionic components and carbonaceous materials are compared in Figure 5. As expected, the total PM_{2.5} mass concentration is higher than the sum of ionic components measured by the URG-9000, but they correlate well. Components of PM_{2.5} such as crustal and carbonaceous materials (the sum of NVOM and BC) are not captured by URG-9000. The difference between total PM_{2.5} and sum of the inorganic ions and carbonaceous material was attributed to SVOM. A good ion charge balance was observed as indicated by the measured and calculated ionic components based on the measured nitrate and sulfate. This finding is consistent with the observation of Kuprov et al. ¹³ and indicates that nitrate and sulfate in fine particulate matter are present as ammonium nitrate and ammonium sulfate, respectively.

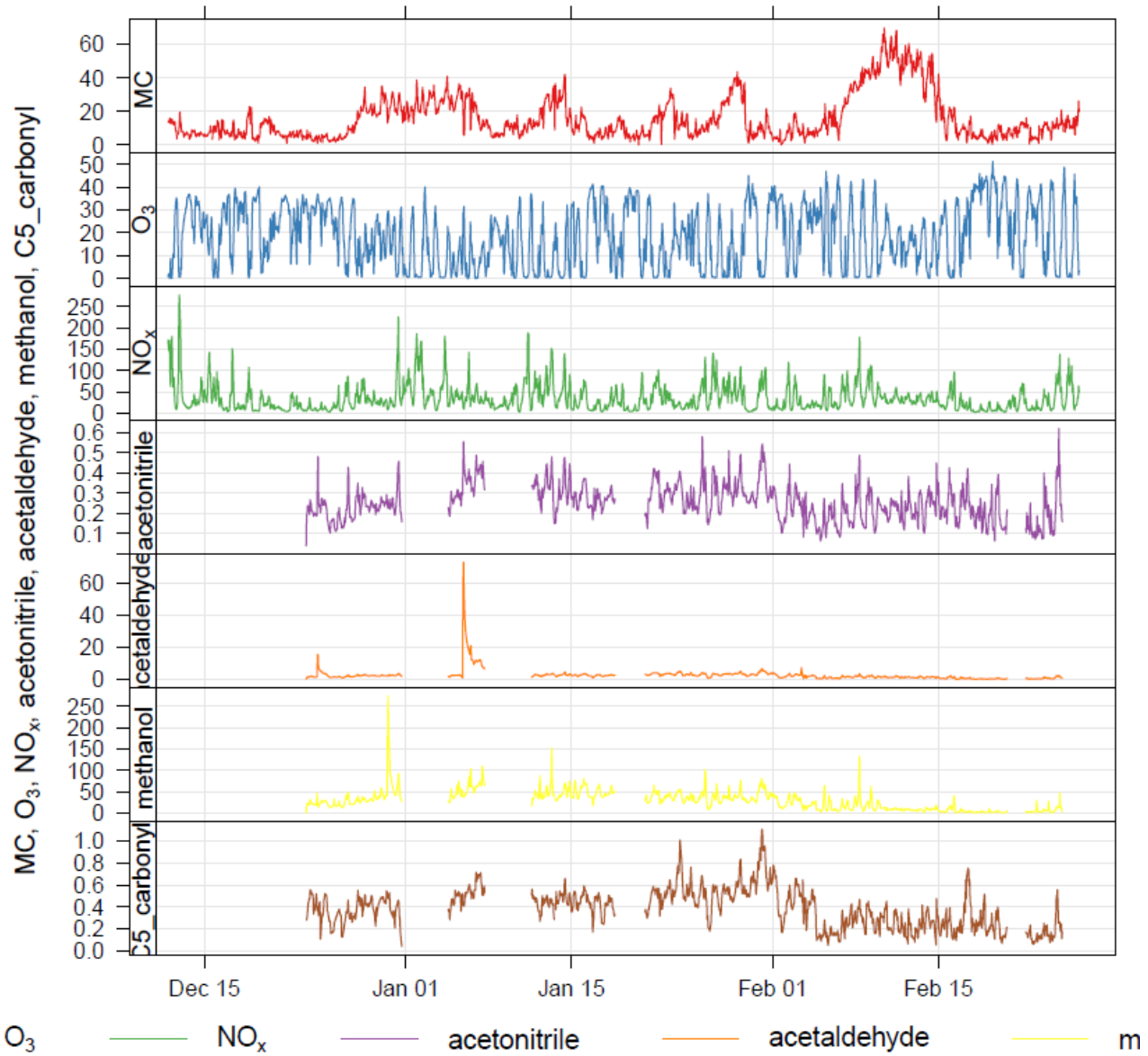


Figure 4: Time series of PM_{2.5}, O₃, NO_x, and example VOCs observed at NAA during the 2015 – 2016 winter.

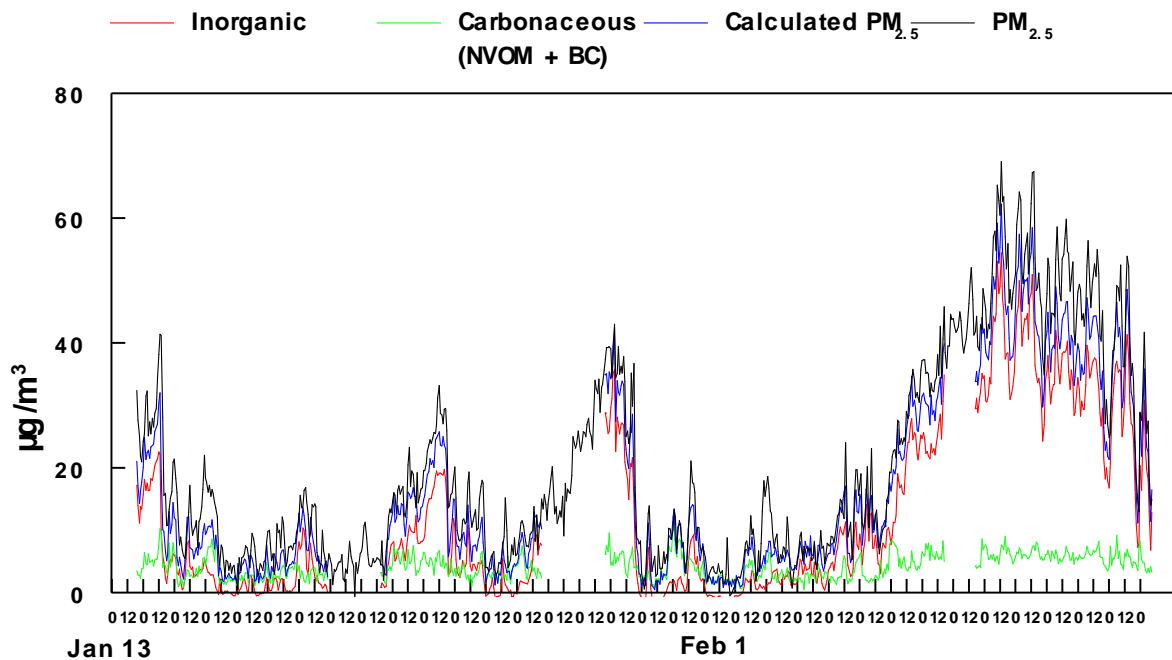


Figure 5 compares the TEOM measurements of $\text{PM}_{2.5}$, Inorganic material (based on the measured nitrate and sulfate assuming they were present as the ammonium salts), the Carbonaceous material (the sum of NVOM and BC) and a calculated $\text{PM}_{2.5}$ concentration calculated as the sum of the inorganic and carbonaceous material during 2015-2016 winter. The difference between the total $\text{PM}_{2.5}$ and the calculated $\text{PM}_{2.5}$ was attributed to SVOM.

In order to examine the importance of the particle bound HAPs, here we compare the chemical composition of fine particulate matter during the clean and polluted conditions. Wintertime particulate composition data was separated into two groups: high-pollution days and clean days as shown in Table 4. High pollution days were defined as those with 24-hr $\text{PM}_{2.5}$ concentrations exceeding $20 \mu\text{g m}^{-3}$. Only the days for which URG-9000 had 24-hr valid samples (midnight to midnight) were used in this analysis (see Table 4).

Table 4 lists polluted and clean days used to determine the PM_{2.5} chemical composition.

Polluted Days		Clean	
12/29/2015	2/6/2016	12/18/2015	1/31/2016
12/30/2015	2/7/2016	1/11/2016	2/1/2016
12/31/2015	2/8/2016	1/14/2016	2/2/2016
1/1/2016	2/10/2016	1/15/2016	2/3/2016
1/2/2016	2/11/2016	1/16/2016	2/4/2016
1/3/2016	2/12/2016	1/17/2016	2/5/2016
1/4/2016	2/13/2016	1/18/2016	2/16/2016
1/23/2016	2/14/2016	1/19/2016	2/17/2016
1/27/2016	2/15/2016	1/21/2016	2/18/2016
		1/22/2016	2/19/2016
		1/24/2016	2/20/2016
		1/25/2016	2/21/2016
		1/30/2016	

The composition of PM_{2.5} during clean and polluted conditions in winter is shown in Figure 6. PM_{2.5} mass concentration is dominated by inorganic aerosols, ammonium nitrate (NH₄NO₃) to be specific, which accounts for 60 – 80% of the total during the pollution episodes and ~ 44 - 58 % outside the pollution episodes. Contribution of carbonaceous material (NVOM + BC) was ~29 % and 20 % on clean and polluted days, respectively, indicating importance of the inorganic aerosols during the pollution episodes. SVOM, derived as a difference between TEOM PM_{2.5} and sum of inorganic and carbonaceous materials, accounts for 20% and 15%, respectively, during clean and polluted periods. Any missing mass, arising from various sampling artifacts such as loss on the sampling lines and volatilization is therefore included as SVOM.

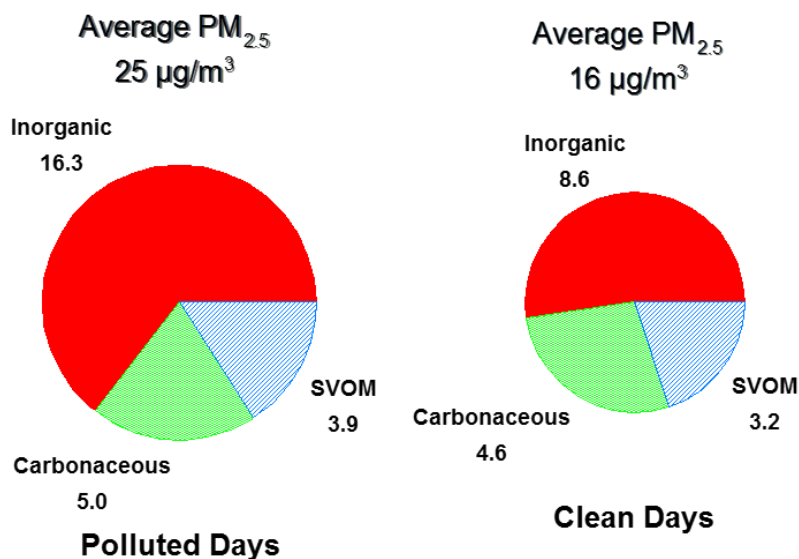


Figure 6: PM_{2.5} mass composition during and outside the pollution episodes during the 2015-2016 winter.

5.1.2. Summer Campaign

A similar suite of gas and particulate species was monitored during the summer campaign although the excessive heat, rain, and other environmental factors affected the quality of measurements related to the particulate matter. Figure 7 provides an overview of the summer observations, indicating lower levels of PM_{2.5} and primary pollutants including NO_x, VOCs (e.g. BTEX species, OVOCs), and higher secondary species such as O₃ in summer compared to winter. PM_{2.5} levels remained low below 10 µg m⁻³ most of the summer except few exceptional events e.g. August 4 – 5 2016 wild fire event that lead to hourly PM_{2.5} of 37 µg m⁻³ (Figure 17). Because of the non-ideal measurement conditions and low levels of PM_{2.5} in summer months, the levels of particulate bound organic species and inorganic ions were often below the detection limit of OAM and URG 9000 analyzers, respectively. Trace gas analyzers were operational and online except the PTR-MS analyzer, which was not operational at the beginning of the campaign due to high ambient temperatures.

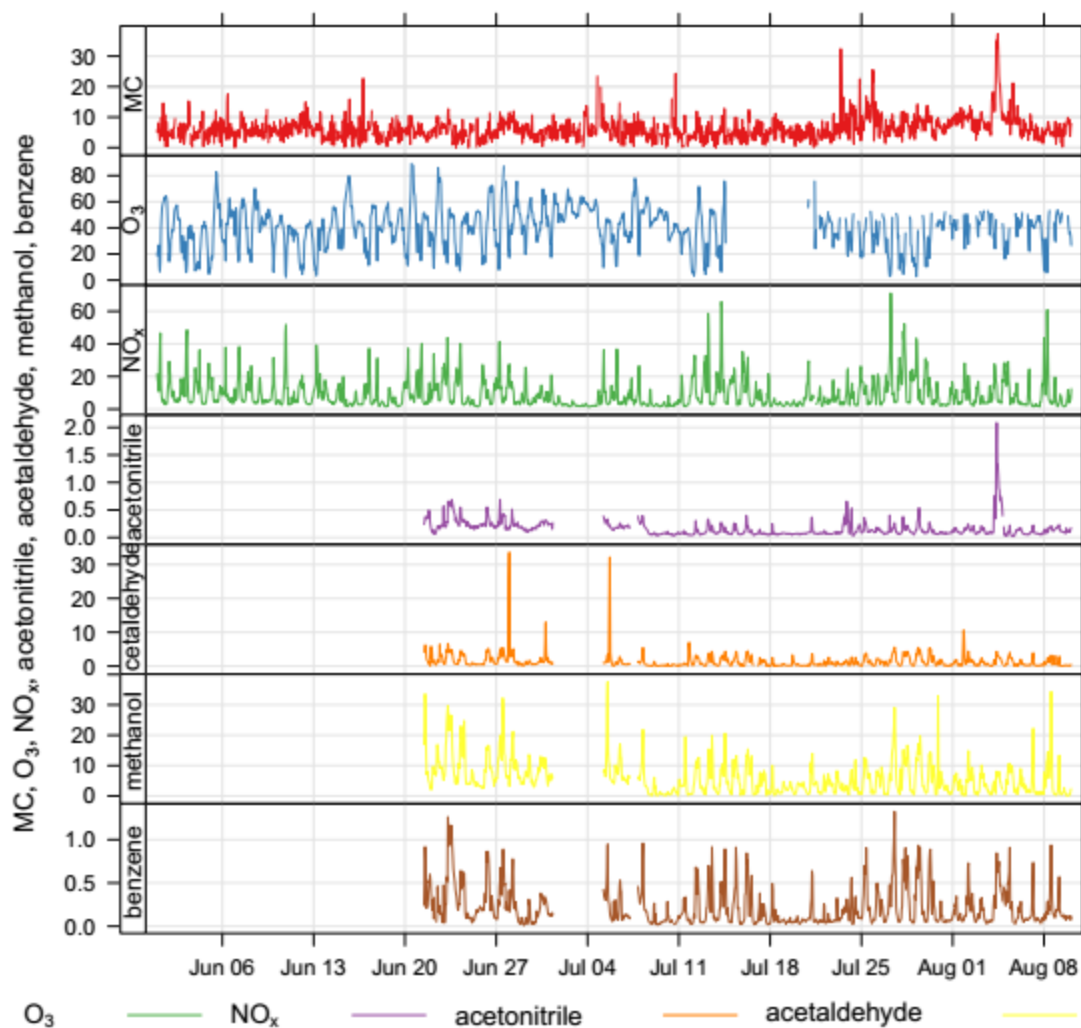


Figure 7: Time series of $PM_{2.5}$, O_3 , NO_x , and example VOCs observed at NAA during the 2015 – 2016 summer

The summertime composition of $PM_{2.5}$ is shown in Figure 8. Ammonium continued to be the dominant ionic fraction in summertime $PM_{2.5}$ contributing 35% to the total ion mass. Bromide, sodium, and nitrite together contributed to the nearly 50% of total $PM_{2.5}$. The rest, 15% of the ionic mass consisted of sulfate, nitrate, potassium, calcium, and chloride indicating the secondary ammonium nitrate and sulfate are not as important in summer months as they are in winter. Instead, bromide and nitrate ions appear to be neutralized by the ammonium ion and the crustal elements including sodium, potassium, and calcium, which constitute ~ 20 % of the total $PM_{2.5}$ in summer months.

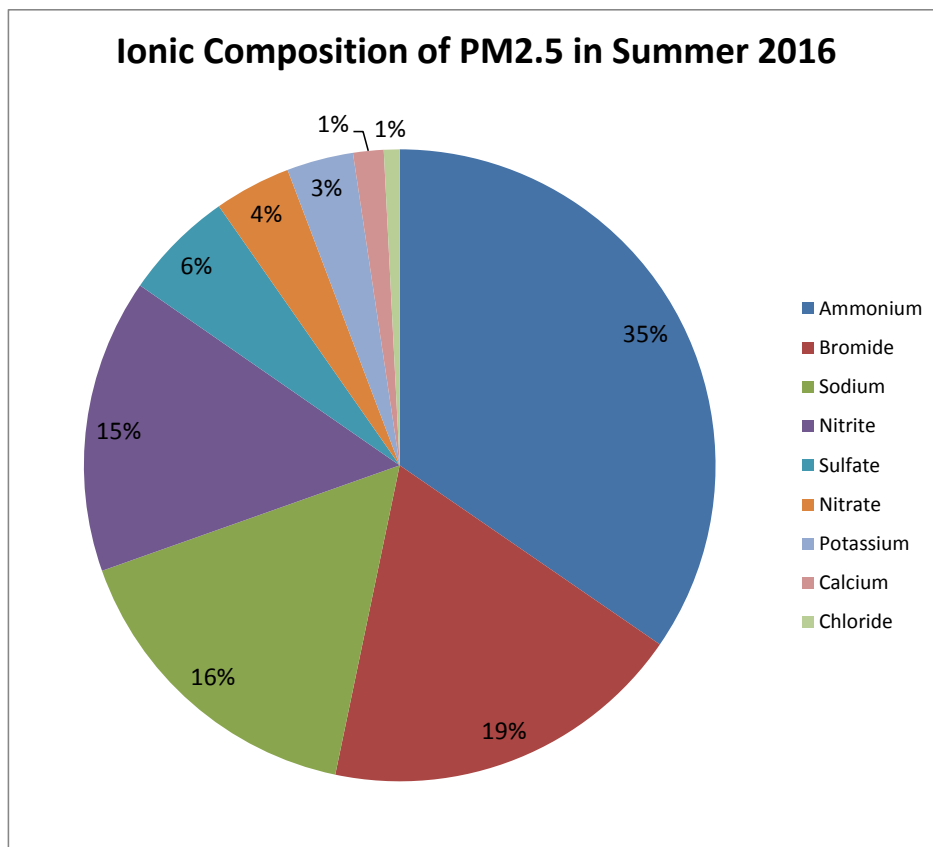


Figure 8: Ionic composition of PM_{2.5} during summer 2016. The total represents the ionic mass only and omits mass contribution from carbonaceous and crustal fractions.

5.2. Source Apportionment Analyses

This section provides details of the analyses conducted as part of this project to characterize the sources of the observed HAPs and presents a) the temporal and spatial variability of BTEX compounds and OVOCs b) Positive Matrix Factorization (PMF) analysis of winter data, and c) the back-trajectory analysis of the events associated with elevated OVOCs.

5.2.1. Temporal and spatial variability

BTEX compounds. Figure 9 shows the ambient levels of benzene, toluene, C8 and C9 aromatics observed at NAA during the winter when the BTEX levels tend to be highest due to the shallow boundary layer and the slow chemical loss processes²². The BTEX levels ranging up to 2 - 4 ppb were observed at this site with the highest peaks occurring during winter pollution episodes. The BTEX levels are lower in the summer months as result of efficient photochemistry (Figure 10). BTEX compounds show a strong diurnal pattern with early morning peak at ~ 7 AM during the winter (Figure 11). Their levels remain low level during the day and show slight enhancement at night due to the shallow nocturnal boundary layer. Wintertime observations were used to make these plots. It is important note that the analysis of summertime data yields consistent results, except the morning peak that occurs ~ 6 am during the summer. The polar plots of the concentrations as a function of wind direction and speed indicate that the highest TBEX levels are associated with easterly, southeasterly winds during the day and easterly at night as shown in Figure 11, that bring pollutants emitted along the Bangerter

highway and I-215. The observed diurnal pattern and pollution rose are consistent with those of CO and NO_x, indicating the predominant contribution of the mobile sources to the observed BTEX levels at this site during winter and summer months. The results of the PMF analysis support this as discussed below (see Table 5).

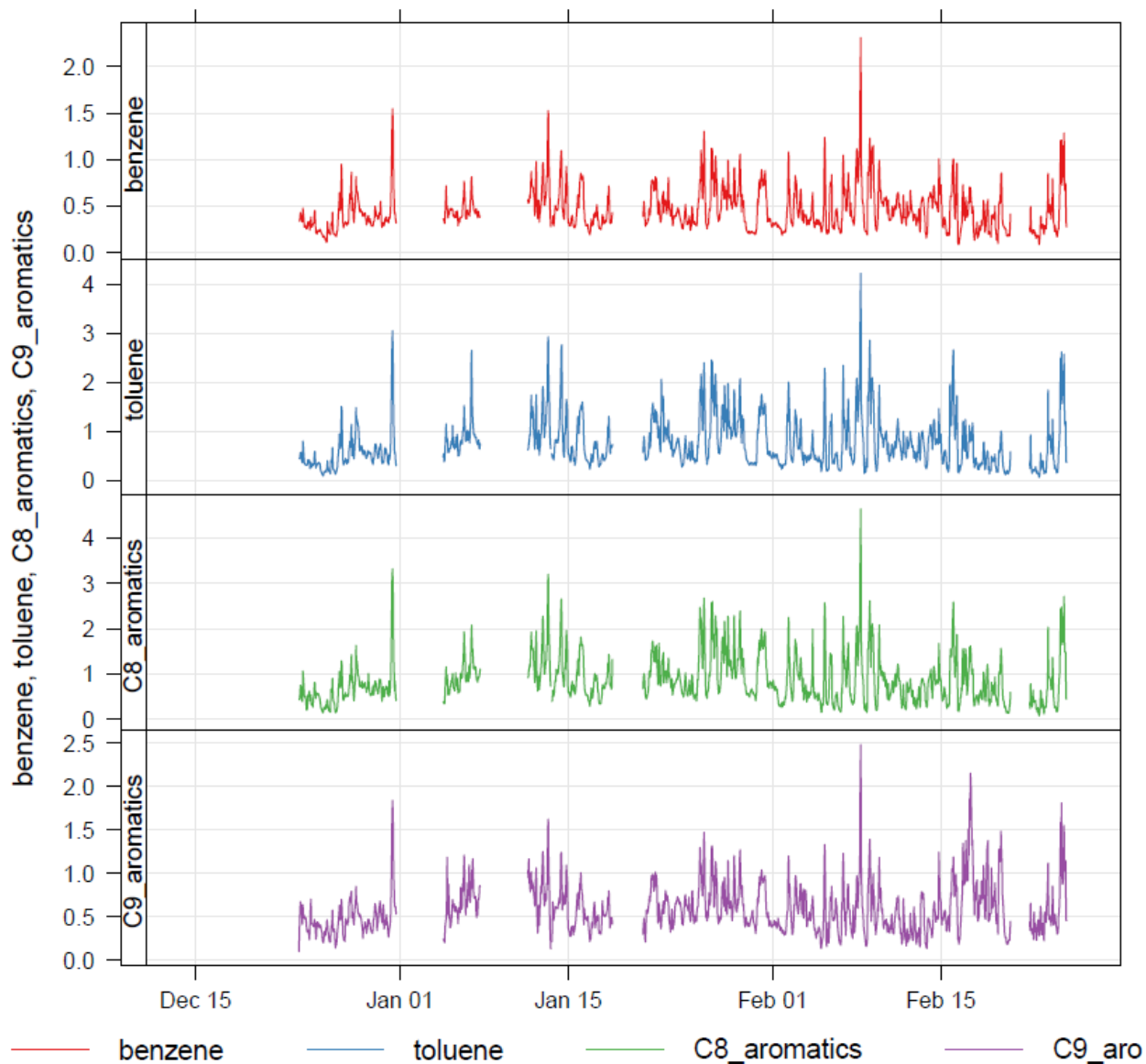


Figure 9: Time series of benzene, toluene, sum of C8 and C9 aromatics measured at NAA during the 2015-2016 winter campaign.

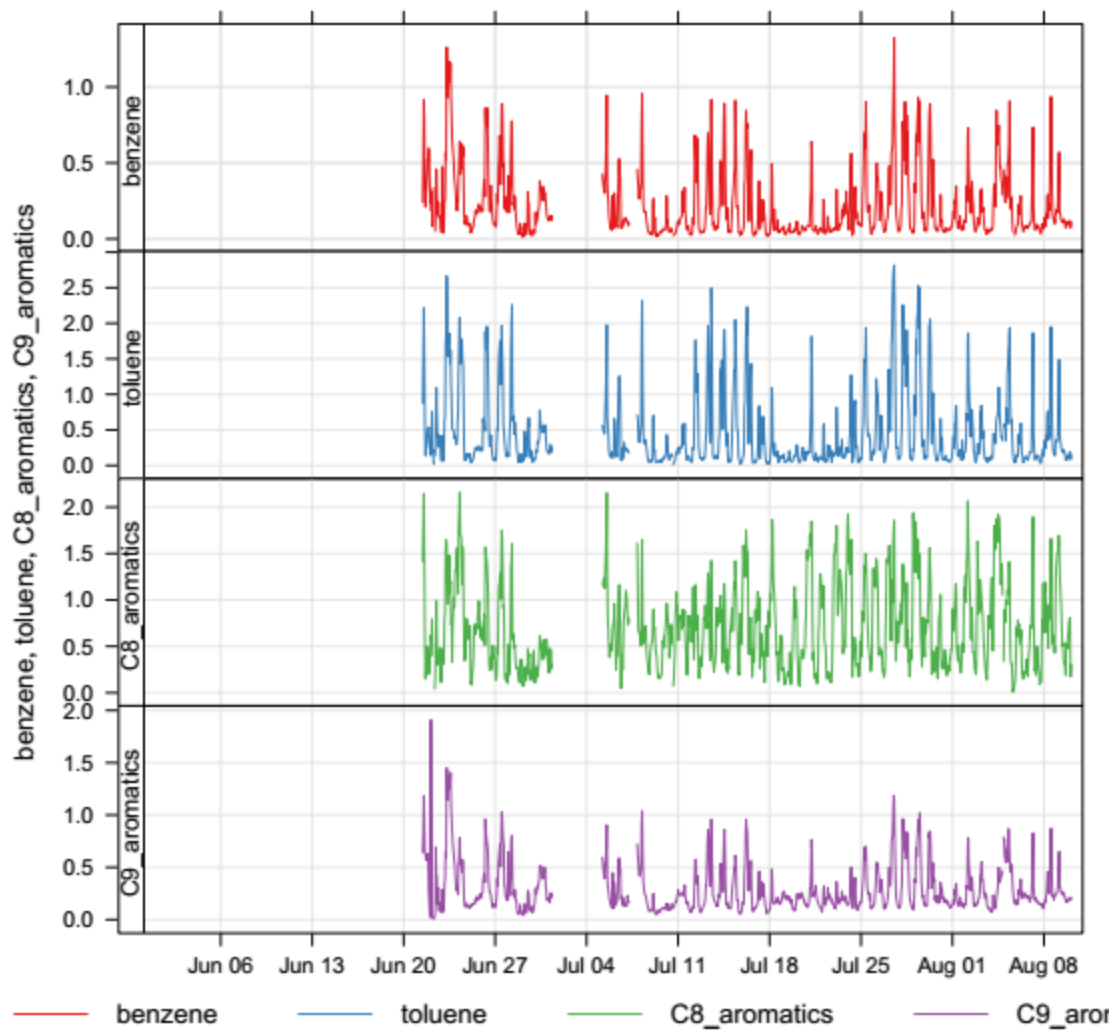


Figure 10: Time series of benzene, toluene, sum of C8 and C9 aromatics observed at NAA during the 2016 summer campaign.

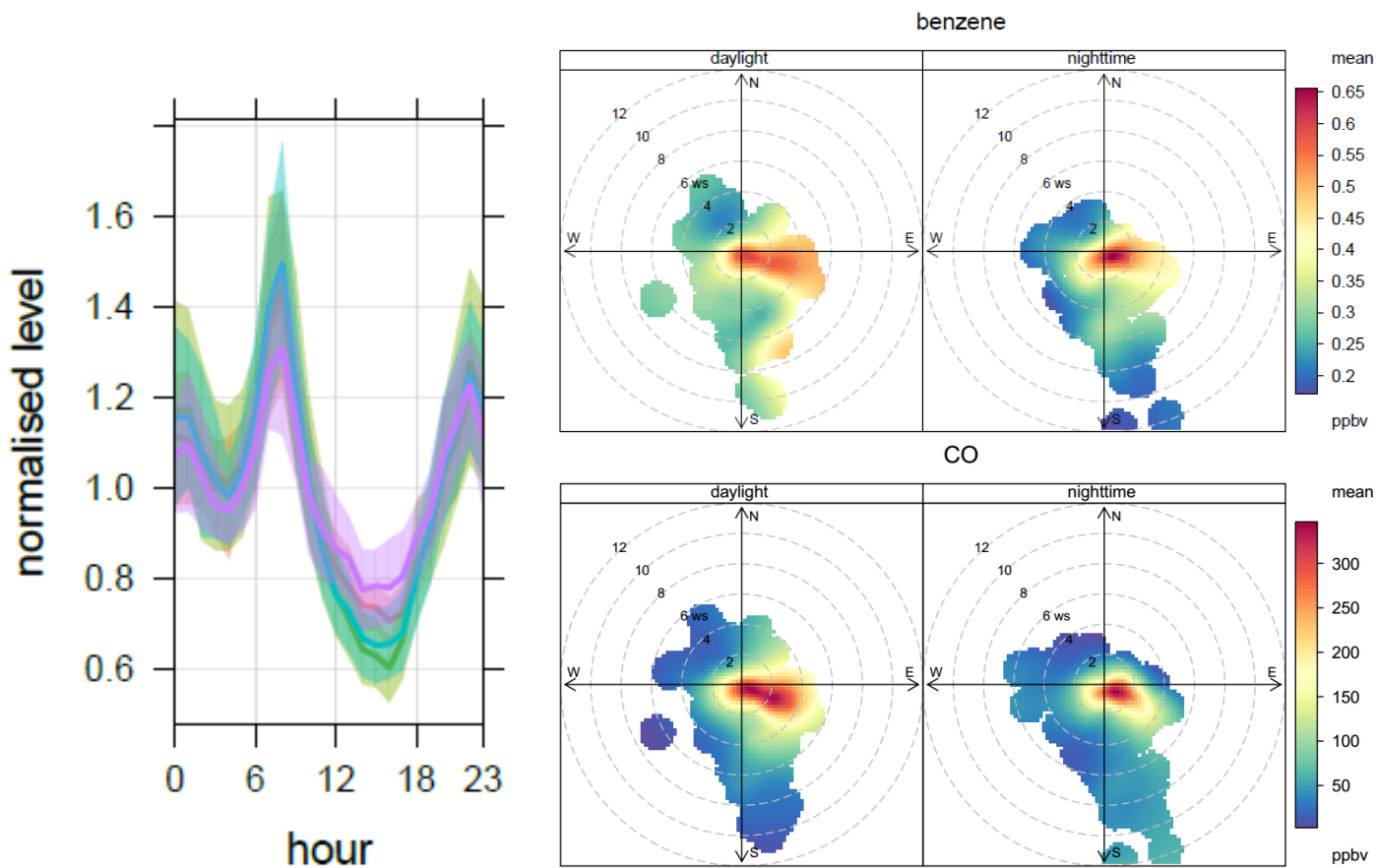


Figure 11: The diel and polar plots of BTEX compounds show signatures associated with on-road sources and indicate the highest concentrations under easterly and southerly winds.

OVOCs. The PTR-MS measurements represent one of the first real-time observations of OVOC's in the SLV. The monitored species include aldehydes (HCHO and CH₃CHO), CH₃OH, carboxylic acids (CHOOH, CH₃COOH), and carbonyl (CH₃COCH₃, methylethylketone (MEK), 3-hexanone). Figure 12 and 13 show summer and winter observations of key OVOC's. In contrast to the BTEX compounds that remain below 2 – 4 ppb and show a morning maxima, OVOCs exhibit different behaviors with some species showing periodic enhancements at night while some show signatures associated with on-road emissions. These enhancements are not associated with the periods of atmospheric stability that occurs typically in winter months, and can occur under both clean and polluted (high PM_{2.5}) conditions. Figure 12 show time series of OVOCs during the winter to highlight the correlation between the observed aldehydes and HCOOH/Dimethyl ether (DME) concentrations. In contrast, CH₃COOH, CH₃OH and CH₃COCH₃ exhibit different trends suggesting a wide array of OVOC sources in the SLV as discussed below in detail.

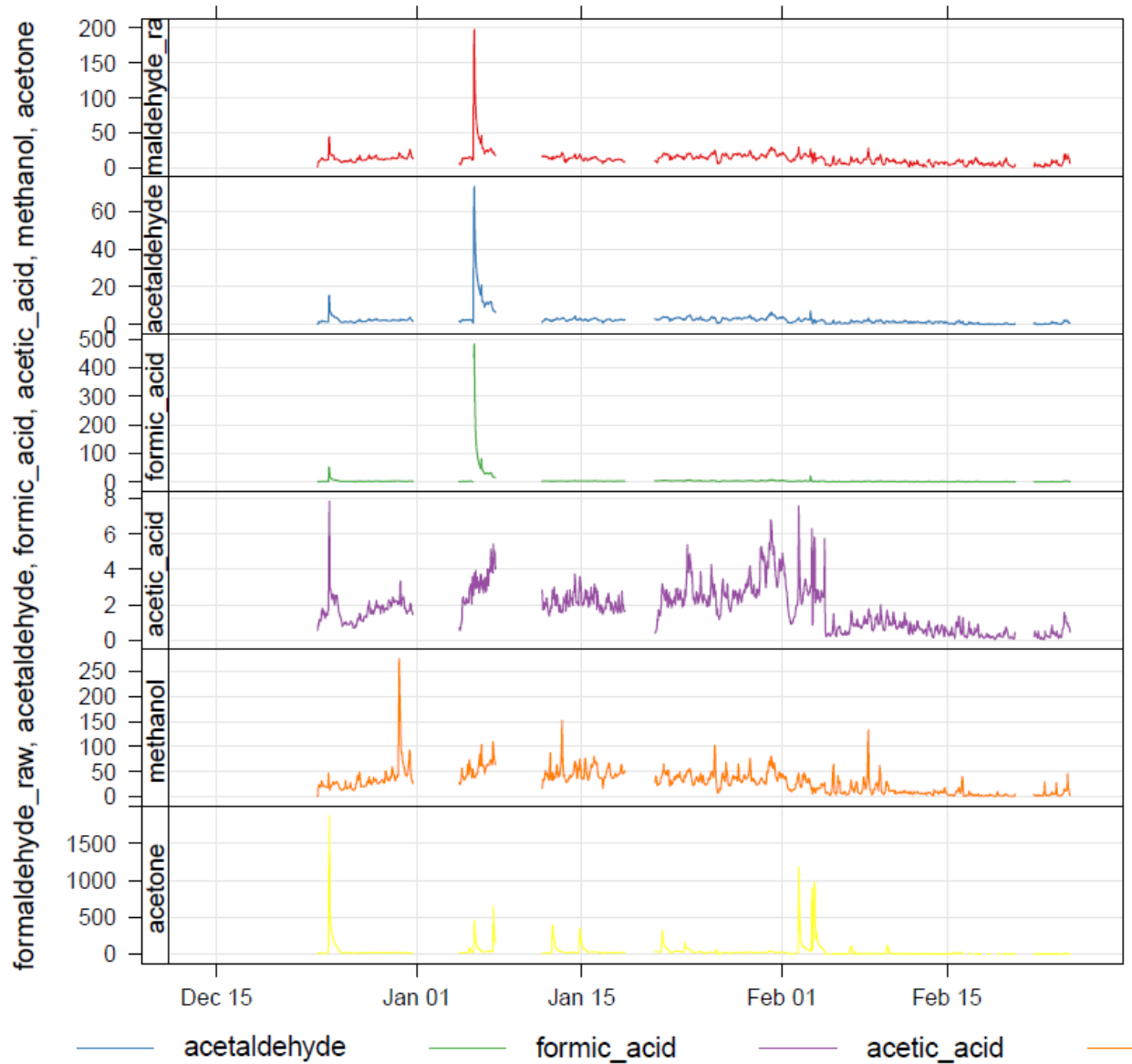


Figure 12: Time series of HCHO , CH_3CHO , HCOOH , CH_3COOH , CH_3OH , and CH_3COCH_3 at NAA during the 2015-2016 winter.

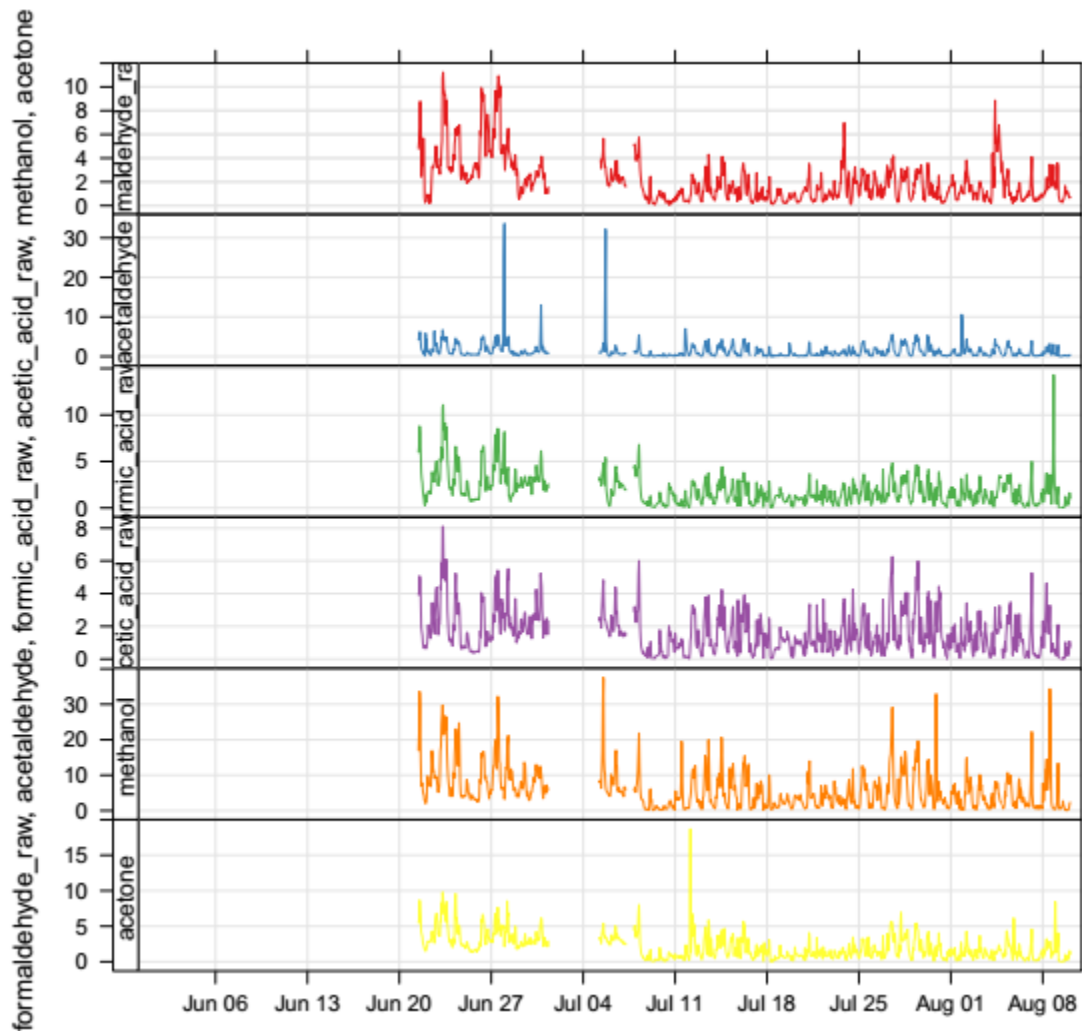


Figure 13: Time series of HCHO , CH_3CHO , HCOOH , CH_3COOH , CH_3OH , and CH_3COCH_3 at NAA during the 2015-2016 summer.

HCHO and CH₃CHO. Our observations indicate periodic, spontaneous emissions of these species (Figure 13) that can lead to 1-hr CH₃CHO levels up to 70 ppb and estimated HCHO levels reaching up to ~ 100 – 200 ppb in winter months. Summer observations also indicate spontaneous enhancements in CH₃CHO and HCHO although the observed levels are lower likely due to deeper boundary layer, efficient mixing

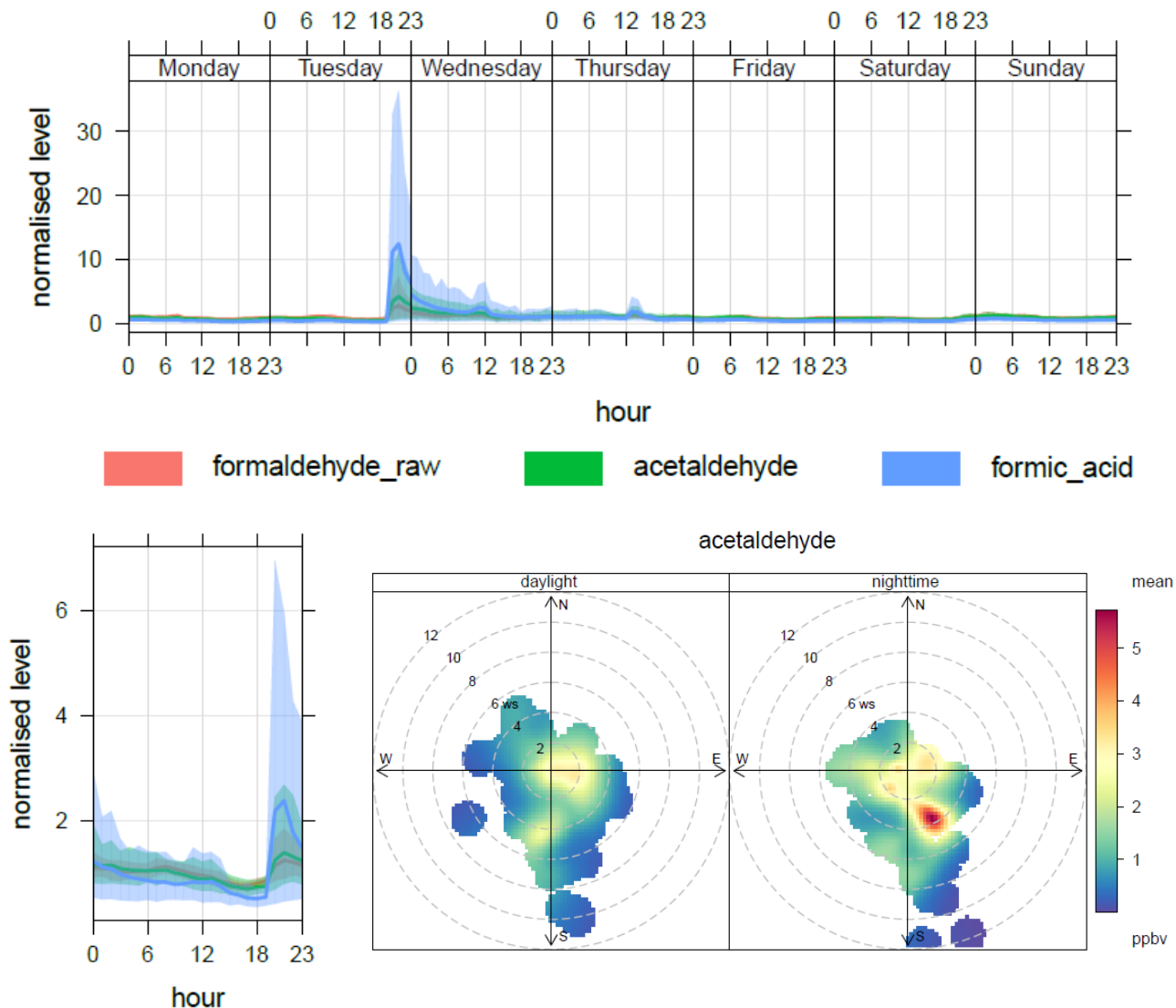


Figure 14: Temporal and spatial variability of HCHO, CH₃CHO and HCOOH/DME as a function of day of the week, time of the day and wind speed and direction to show the importance of a source located southeast of NAA that emits at night midweek.

and photochemical loss. This seasonal trend of formaldehyde and acetaldehyde that showed wintertime maximum is consistent with the observation of Kuprov¹¹. It is important to note that the absolute value for HCHO is highly uncertain due to experimental uncertainty discussed in the method section. Nonetheless, these observations suggest sporadic enhancements of HCHO and CH₃CHO that can last for few hours. Concentrations of these species correlate well with each other and with PTR-MS signal at m/z 47, indicating same sources of these species. The PTR-MS signal corresponding to m/z 47 detects HCOOH, DME and CH₃CH₂OH. Due to low PTR-MS sensitivity to CH₃CH₂OH compared to that of

HCOOH, CH₃CH₂OH contribution is expected to be minimum. DME, on the other hand, can be found in urban areas and interfere with PTR-MS HCOOH measurements^{16, 29}. As a result, the signal at m/z 47 is considered as HCOOH/DME assuming their sensitivities are comparable. Both HCOOH and DME are not HAPs, but their emissions appear to be correlated frequently with those of HCHO and CH₃CHO.

The weekly and daily trends indicate sporadic emissions of these species that occur mid week at night as shown in Figure 14. This figure also shows the concentrations of CH₃CHO as a function of wind direction and wind speed as an example. The slight enhancements up to 2-3 ppb observed for CH₃CHO are associated with the easterly winds similar to the patterns of BTEX, NO_x and CO (Figure 11), indicating a small contribution of the on-road sources to the observed CH₃CHO and HCHO, consistent with the diurnal pattern (Figure 15). However, the highest concentrations are observed under southeasterly winds showing evidence of a source of HCHO and CH₃CHO to southeast of the site that release these compounds for a short duration at night during the week. The back trajectory analysis associated with these events are discussed below in section 5.2.3.

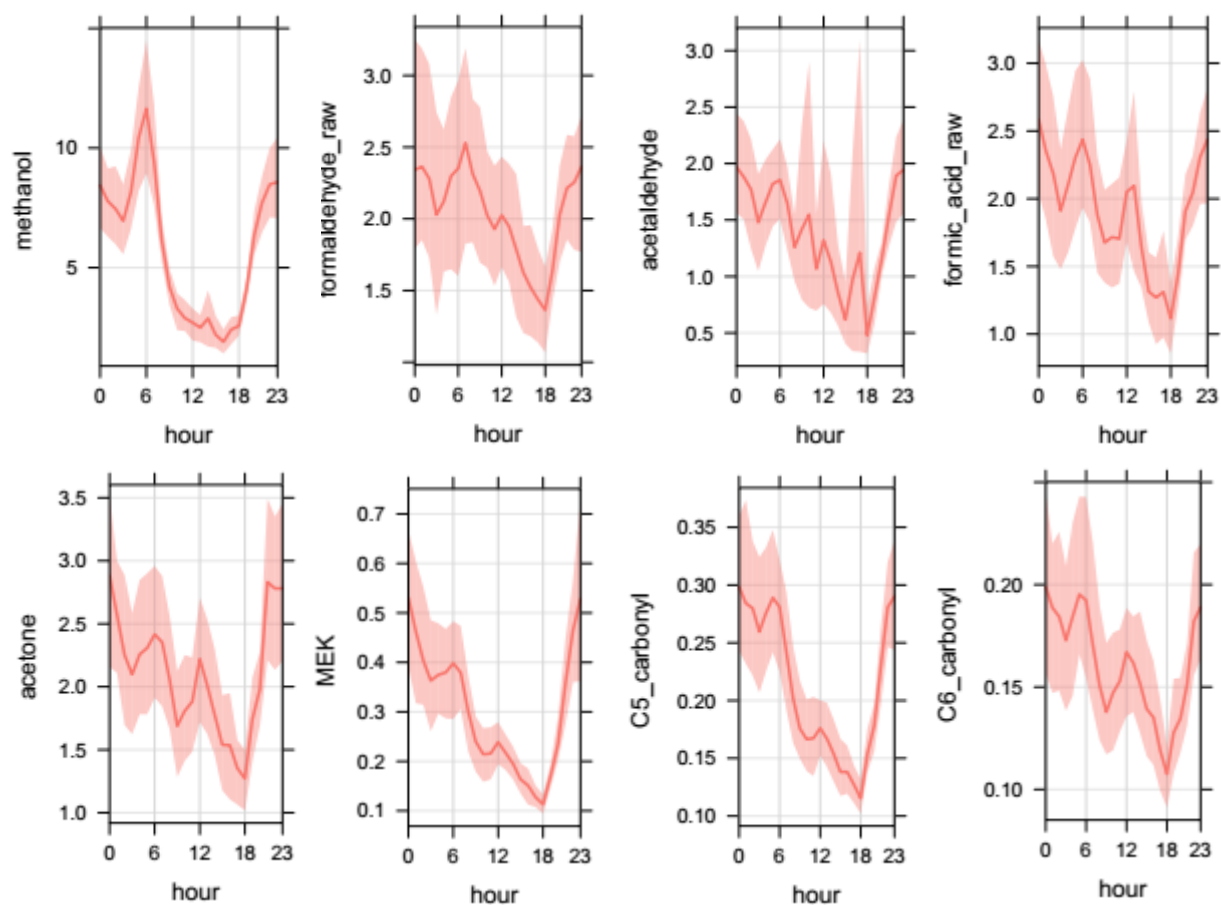


Figure 15: Diel variations of OVOC's observed at NAA during the 2016 summer campaign.

Figure 15 shows diurnal trends of key OVOCs observed in summer months. The summertime observations of these aldehydes and ketones indicate a slight enhancement midday consistent with the

photochemical production of these species. It also highlights that photochemical contribution to the observed CH_3CHO , HCHO , CH_3OH and MEK levels is relatively small compared to the anthropogenic contribution. In contrast, acetone, C6 carbonyls, acetic and formic acid levels are influenced by the photochemical production more as indicated by a noticeable midday peak.

CH_3OH and CH_3COCH_3 . CH_3OH levels reaching up to 250 ppb with wintertime seasonal mean of 28.6 ppb were observed at NAA. Similarly high levels of CH_3COCH_3 reaching up to 1.5 ppm were observed at NAA. Even though both CH_3OH and CH_3COCH_3 are common solvents, their concentrations show different temporal features indicating different sources of these species. Temporal trends of CH_3OH and CH_3COCH_3 are compared in Figure 16.

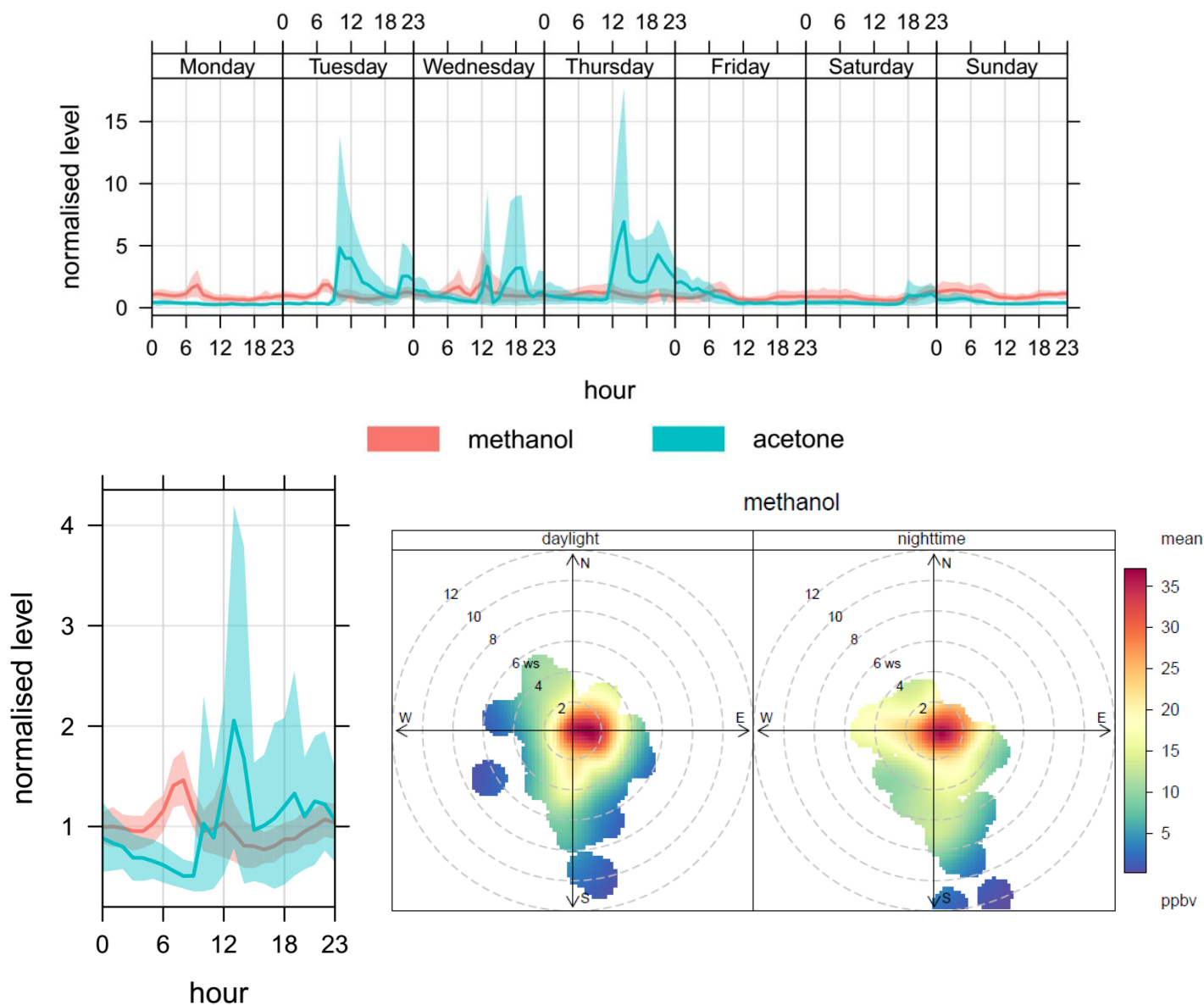


Figure 16 comparing the temporal variability of CH_3OH and CH_3COCH_3 to highlight different sources of these species. Diurnal patterns and the polarplots of CH_3OH show its association with on-road emissions.

Both species show higher values midweek, however their diel patterns are significantly different as shown in Figure 16. CH_3OH exhibits features similar to BTEX, NO_x and CO, with an early morning peak and enhancements under easterly winds. This indicates the main source of CH_3OH at this site is the emissions from the mobile sources, consistent with findings of PMF analysis discussed below (Section 5.2.2 and Table 5). The highest peaks of CH_3OH were observed during the periods of atmospheric stability.

In contrast, CH_3COCH_3 levels show sporadic enhancements during the day midweek under southerly winds indicating industrial activities located south of the site that use and release acetone. These peaks are seldom associated with those of HCHO and CH_3CHO , indicating different sources of CH_3COCH_3 .

CH_3CN . CH_3CN (acetonitrile) is one of the HAPs detected by PTR-MS and is often used as a marker for biomass burning^{19, 30}. The concentrations of CH_3CN were low at NAA often ranging between 0.1 – 0.5 ppb as shown in Figure 4 and 7. The highest CH_3CN value of 2 ppb was observed during 4 – 5 August 2016 event when the SLV was influenced by a wild fire plume (Figure 17). However, the level of CH_3CN did not remain elevated for a long time as CH_3CN levels quickly decreased from 2 ppb to 0.5 ppb within 12 hours. As result, the 24-h value for CH_3CN was below 0.6 ppb. Simultaneous enhancements in $\text{PM}_{2.5}$ and HCHO were observed during this event as shown in Figure 17.

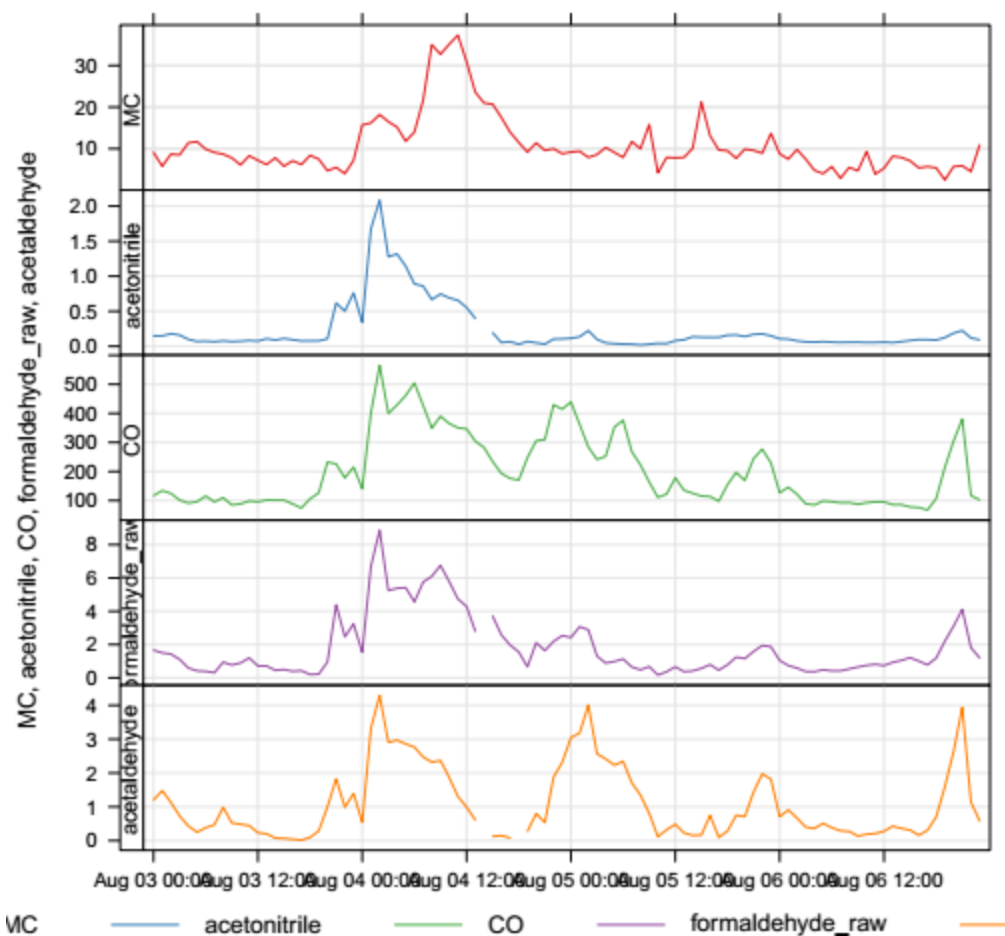


Figure 17: Enhancements in $PM_{2.5}$, CH_3CN , CO , and CH_3CHO levels observed during August 4 – 5 2016 wild fire event.

Low CH_3CN levels observed in winter months indicated a minor influence of biomass burning at this site as further supported by PMF analysis (section 5.2.2), which estimated the woodsmoke contribution to the total $PM_{2.5}$ to be $\sim 3.5\%$ on average during the winter.

5.2.2. PMF analysis for Source Apportionment

Complete data were available for the PMF analysis for the time period from 16:00 January 13 through 19:00 January 19, 12:00 January 21 through 16:00 January 26, 17:00 January 28 through 14:00 February 2 and 14:00 February 9 through 23:00 February 15, 2016, providing 689 data sets for the PMF analysis reported here. A total of 23 species were present in each of the data sets. The data are given in Figures 18 – 20.

PMF analysis was conducted investigating the results assuming from 4 to 9 factors discussed in the method section. After examining the results from the various analyses, it was observed that three components consistently gave results, which reflected little predicted mass, and contribution from essentially only the component. These components, ozone, pyrene and anthracene were dropped from consideration in the final analyses. The resulting data were best described with 5 factors. The final PMF

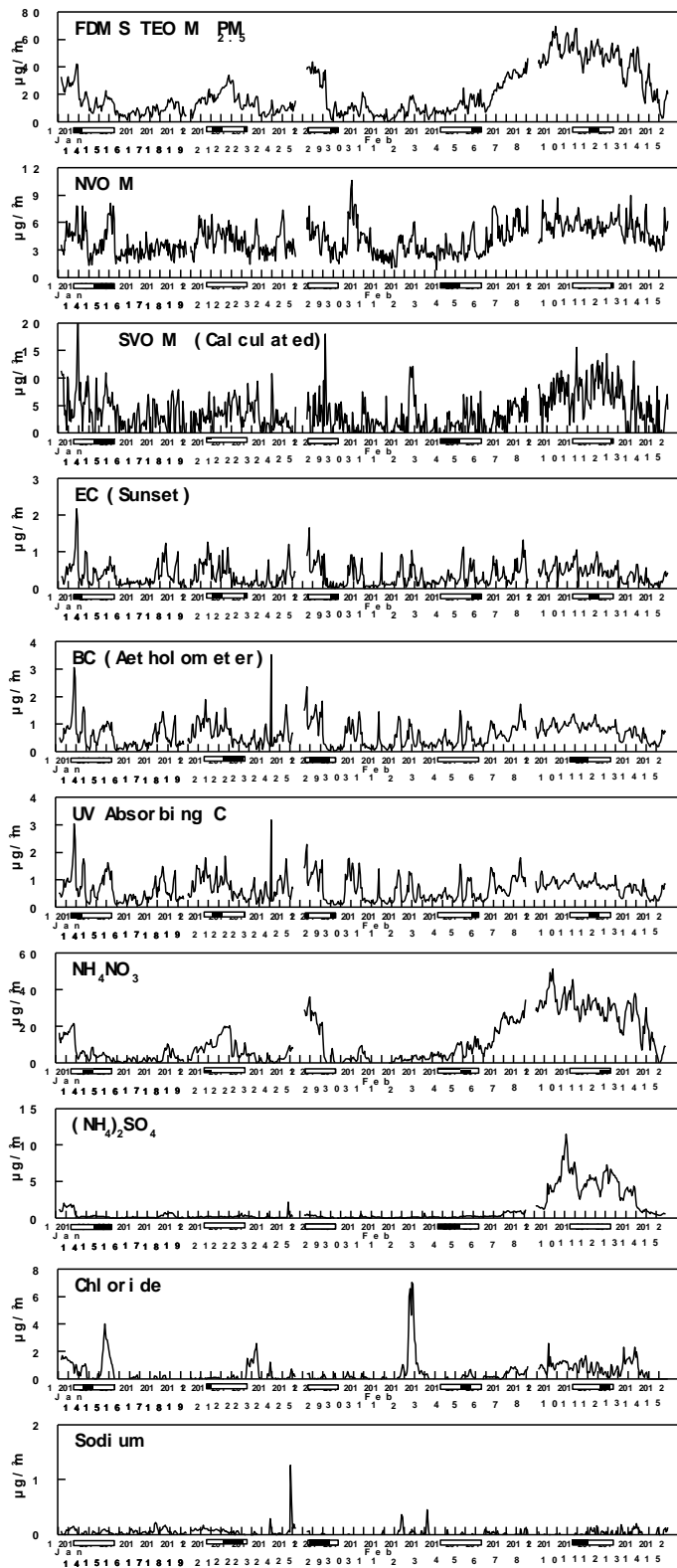


Figure 18: PM_{2.5} and particulate chemical composition data used in the final PMF analysis. Weekends are noted with a crosshatch bar below the X axis.

solution was further analyzed using the “key” option of PMF to optimize the description of the major PM

components (but not the assignment of the various minor aerosol marker species). The comparison of measured and PMF predicted mass is shown in Figure 21 with the time series for each factor shown in Figure 22 and the associated profiles given in Table 5. A pie chart of the results is given in Figure 27.

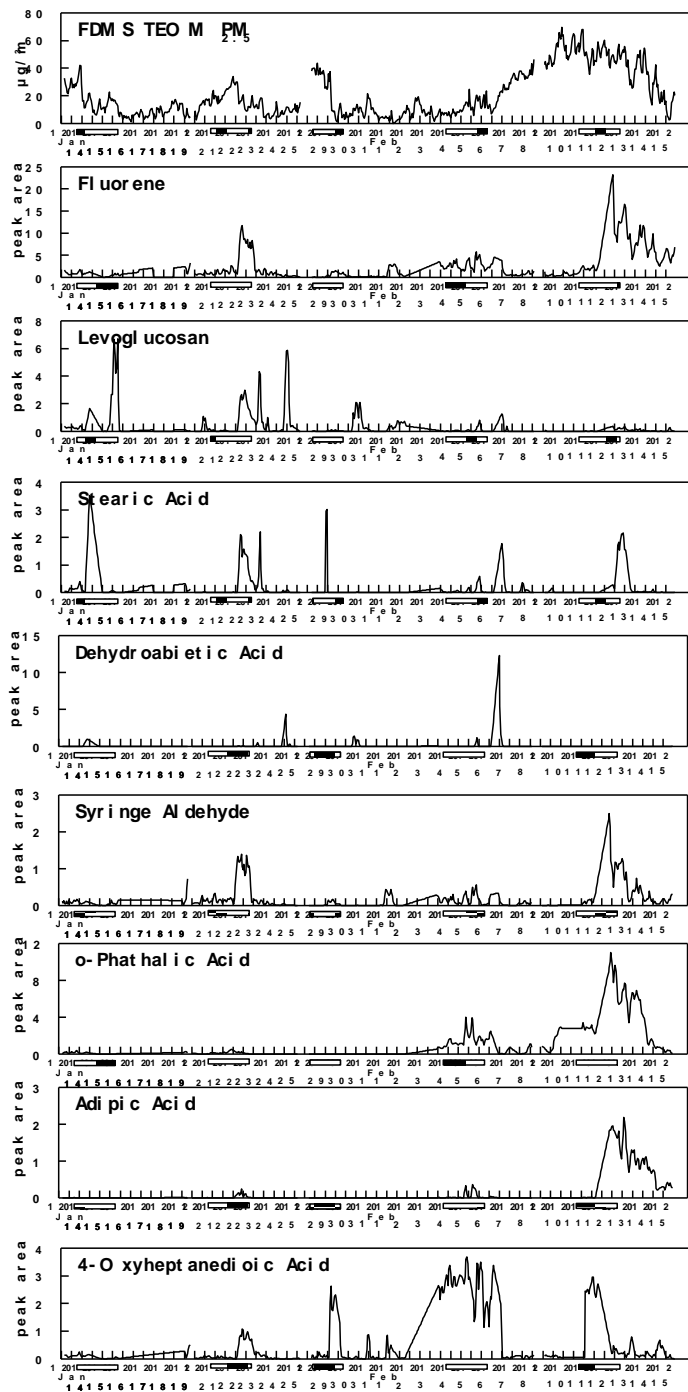


Figure 19: $\text{PM}_{2.5}$ and particulate organic marker data used in the final PMF analysis. Weekends are noted with a crosshatch bar below the X axis.

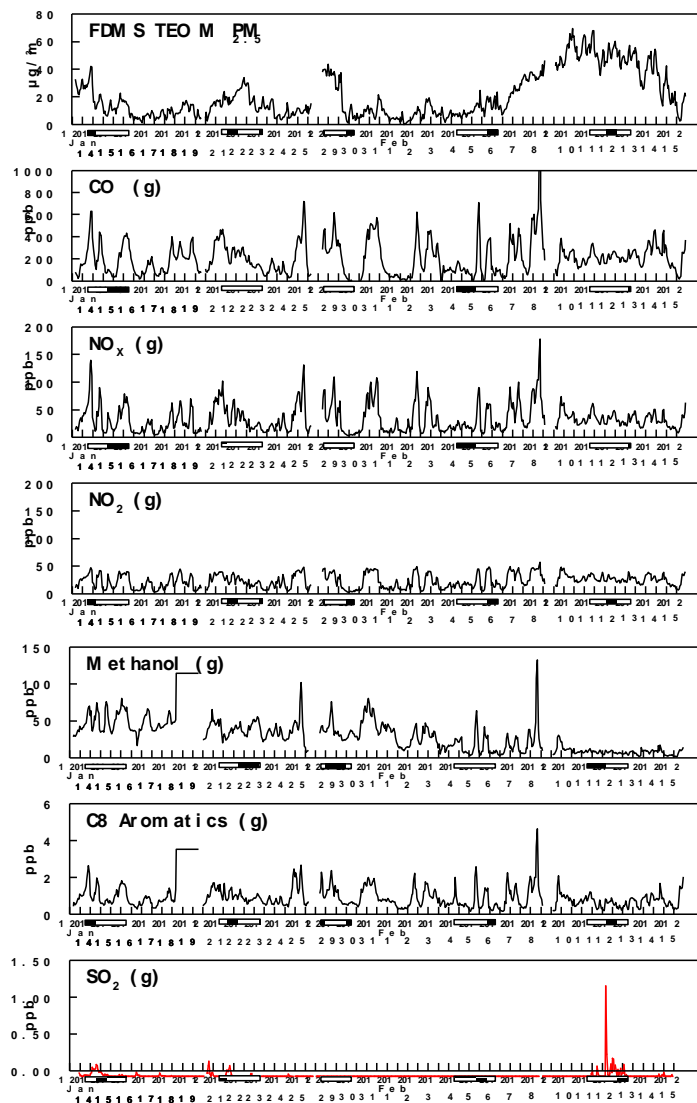


Figure 20: $PM_{2.5}$ and gas phase data used in the PMF analysis. SO_2 data is given in red because it was used to interpret the PMF analysis, but was not used directly in the analysis. Weekends are noted with a crosshatch bar below the X axis.

Discussion of Each Factor Identified in the PMF Analysis

Factor 1 is present an average of $2.5 \mu\text{g}/\text{m}^3$. It contains 73% of the CO and 46% of the NO_x . The mass is reasonable well predicted (a ration of components to mass of 0.84) and consists of NVOM, SVOM and BC in the ratio of 0.65:0.15:0.01. The factor is present primarily in the day. These characteristics are all typical of a factor dominated by emissions from gasoline powered vehicles. In addition, the strong presence of C8 Aromatics (71% of the total) and methanol (86% of the total) in the profile are also consistent with this assumption. Factor 1 is assumed to be an auto emissions related factor.

Factor 2 is present an average of $0.6 \mu\text{g}/\text{m}^3$. It contains 41% of the NO_x and 84% of the BC. The mass is over-predicted by the PMF results by a factor of 1.78 and consists of NVOM, SVOM and BC in the ratio of 0.97:0.14:0.90. The mass over-prediction probably results from the relatively small contribution of this factor to the total mass. However, the ratio of NVOM to BC is typical of that expected for diesel

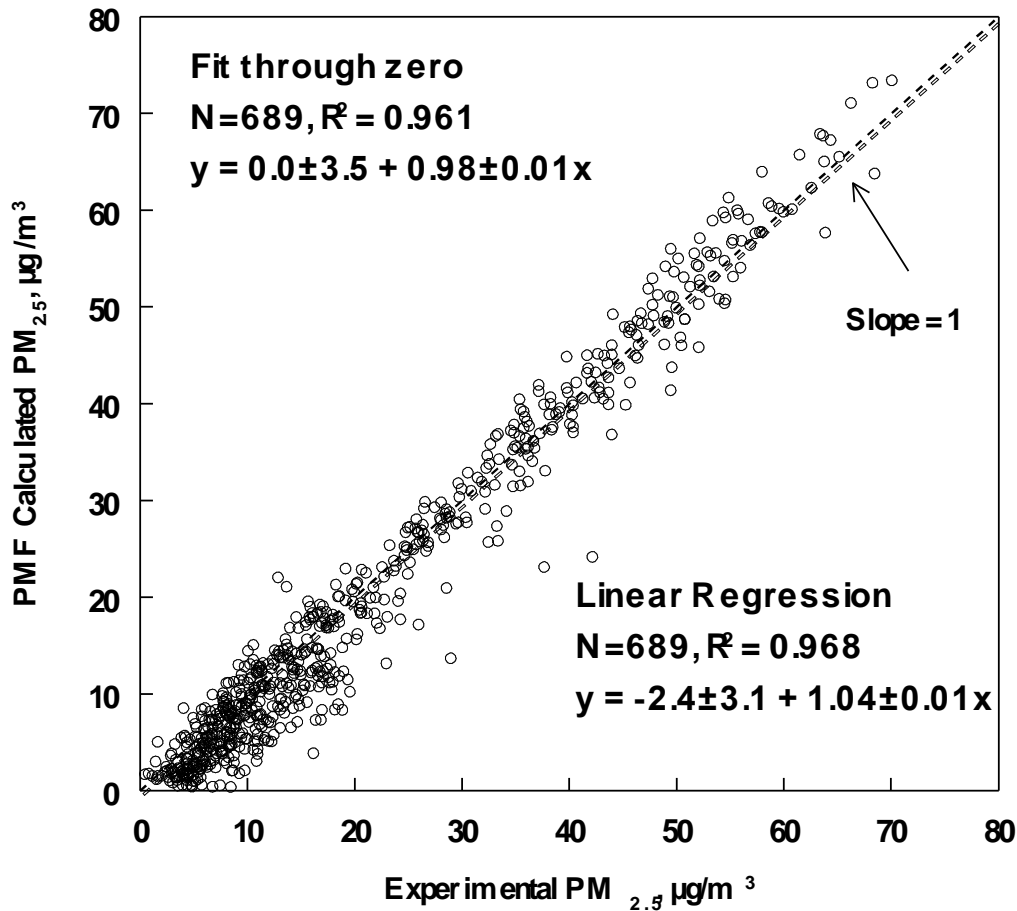


Figure 21: Comparison of the measured and PMF predicted $\text{PM}_{2.5}$ mass.

emissions. These characteristics are all typical of a factor dominated by emissions from the diesel-powered vehicle fleet. In addition, the presence of much of the remaining C8 Aromatics (13% of the total) and methanol (5% of the total) in the profile are also consistent with that assumption. However, the diurnal pattern of $\text{PM}_{2.5}$ does not show the expected morning peak and weekend reduction normally seen for a diesel related factor. This probably reflects that the Neil Armstrong Academy is not near any major traffic ways expected to carry diesel vehicles, which probably also accounts for the low average concentrations of this factor. Factor 2 is assumed to be a diesel emissions related factor.

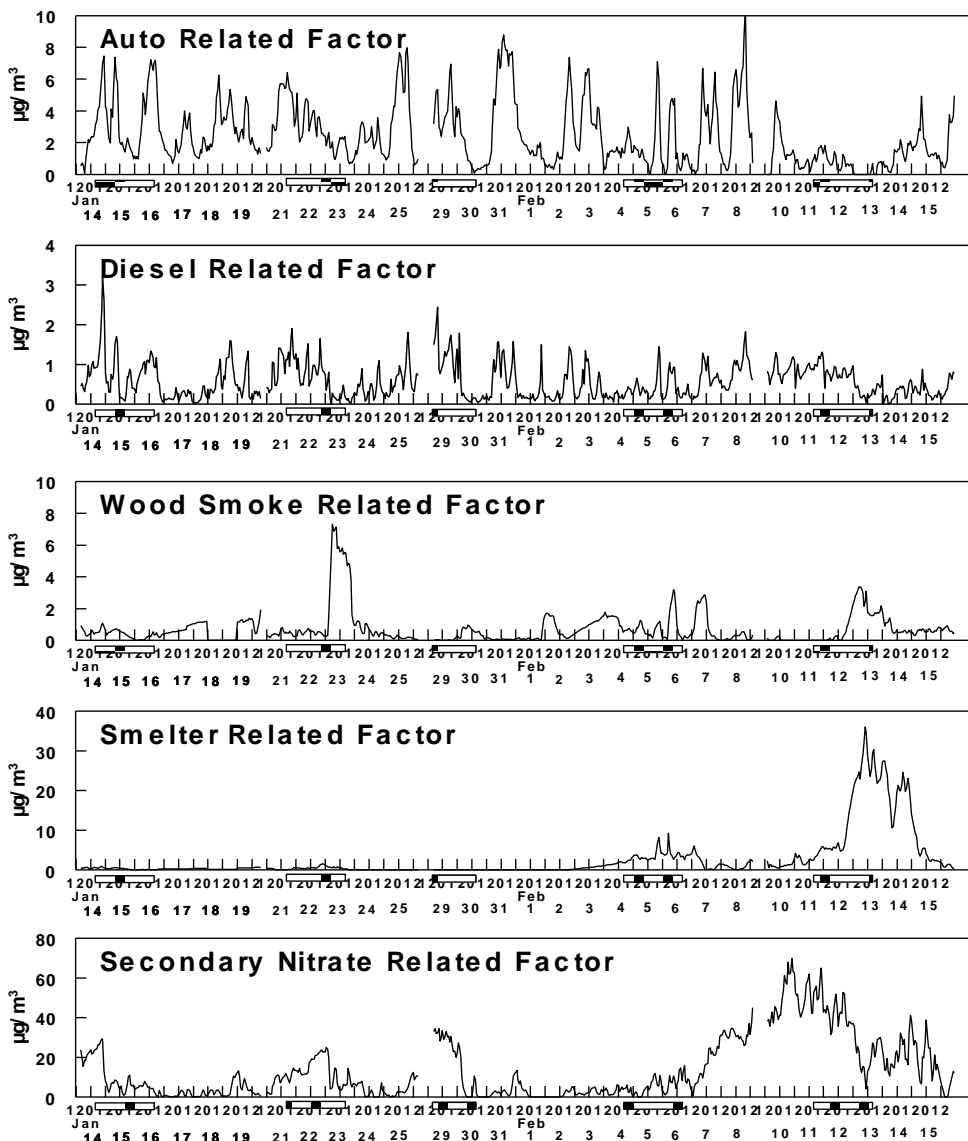


Figure 22: Diurnal variations in the concentrations of the identified 5 factors in the PMF analysis. Note that the Y axis scales are different for each plot. Weekends are noted with a crosshatch bar below the X axis.

Factor 3 is present an average of $0.7 \mu\text{g}/\text{m}^3$, although it is only sporadically present. It is present only in the evening and tends to be present on weekends or Monday night. The mass of the factor is well explained by the PMF results (ratio of components to mass of 0.97). It consists of 53% NVOM, 43% SVOM and 3% BC. These characteristics are all typical of a factor dominated by wood smoke emissions. In addition, the presence of Levoglucosan (97% of the total) and dehydroabietic acid (57% of the total) in the profile are also consistent with this assumption. Furthermore, the occurrence of this factor on Monday nights peaks are consistent with the tradition of members of the Church of Jesus Christ of Latter-day Saints which constitutes a significant fraction of the population in West Valley City to hold a “Family Home Evening” on Mondays. Factor 3 is assumed to be a wood smoke related factor.

Factor 4 is present an average of $2.8 \mu\text{g}/\text{m}^3$, although it is only present in significant amounts during the time period of February 12 -14. The mass of the factor is reasonable well explained by the PMF results (ratio of components to mass of 0.89). It consists of 13% NVOM, 8% SVOM, 5% BC, 52% ammonium nitrate and 14% ammonium sulfate (45% of the total ammonium sulfate). Another strong characteristic of this factor is that it is present in late February concurrent with the highest concentrations of SO_2 (g) seen during the study, Figure 24.



Figure 23: Location of major SO_2 sources in the valley. The emissions rates are annual averages (ton year-1) based on 2014 inventory and represent the entire facility (courtesy of Chris Pennell, UDAQ).

Three major point sources of SO₂ in the area include Kennecott Smelter and Refinery, Kennecott Power Plant and the refineries located in North Salt Lake City (Figure 23), which could contribute to Factor 4. One is the complex of 5 oil and gas refineries located to the northeast of NAA shown in Figure 23. The Chevron Refinery is located just SW of the junction of I-215 and I-15. The Big West Refinery is located northwest of the junction on I-21 and I-15. The Teroso Refinery is 5 mi south of the Chevron refinery on the east side of I-15. There are two refineries north of the Chevron Refinery and both on the west side of I-15, the Silver Eagle Refinery is 5 mile north and the Holly Corporation is 6 miles north. The largest of the refineries are the Tesoro and Chevron operation. Together these refineries emit ~887 tons of SO₂ annually. The second point source is the Rio Tinto Kennecott Smelter located 12 miles west of NAA. Annual SO₂ emissions from the facility are 703 ton/year. However, almost all of these emissions are released from a 1215 foot tall stack and it is not clear how effectively these plumes impact the Salt Lake Valley airshed during wintertime cold pool events, being released at an altitude in the upper part of or above a PCAP. The height of the stable boundary layer varies as a function of time ranging between ~ 400 – 600 m during PCAPs^{1,6}. Fugitive SO₂ emission for Salt Lake and Davis County, which could impact the valley are believed to be about 600 tons/year.

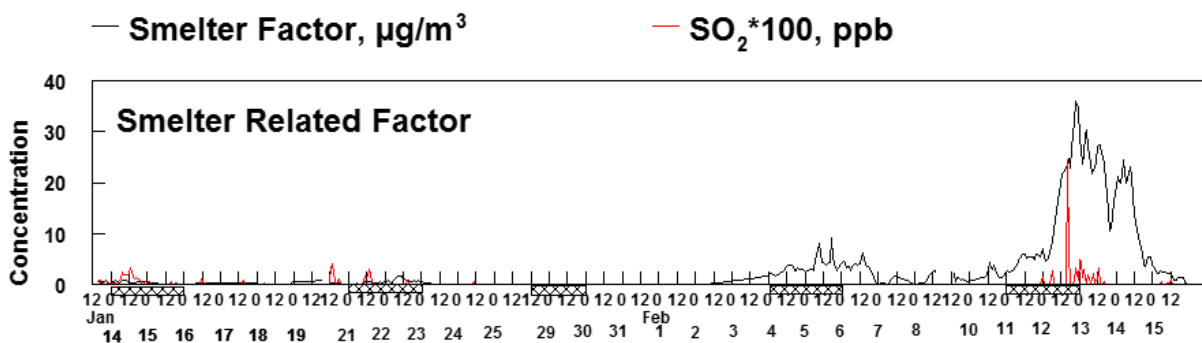


Figure 24: Diurnal pattern of Factor 4 and SO₂ (g).

Figure 25 gives polar plots of SO₂ as a function of wind direction and speed. Wind direction and speed analysis indicates that the levels of SO₂ are highest during the day with westerly and northwesterly winds (Figure 25), which may suggest influence from the Kennecott Smelter and Refinery, and other unreported sources located west of NAA. It is interesting to note that this factor also contains 98% of the o-phthalic acid and 94% of the adipic acid.

Sulfate_G

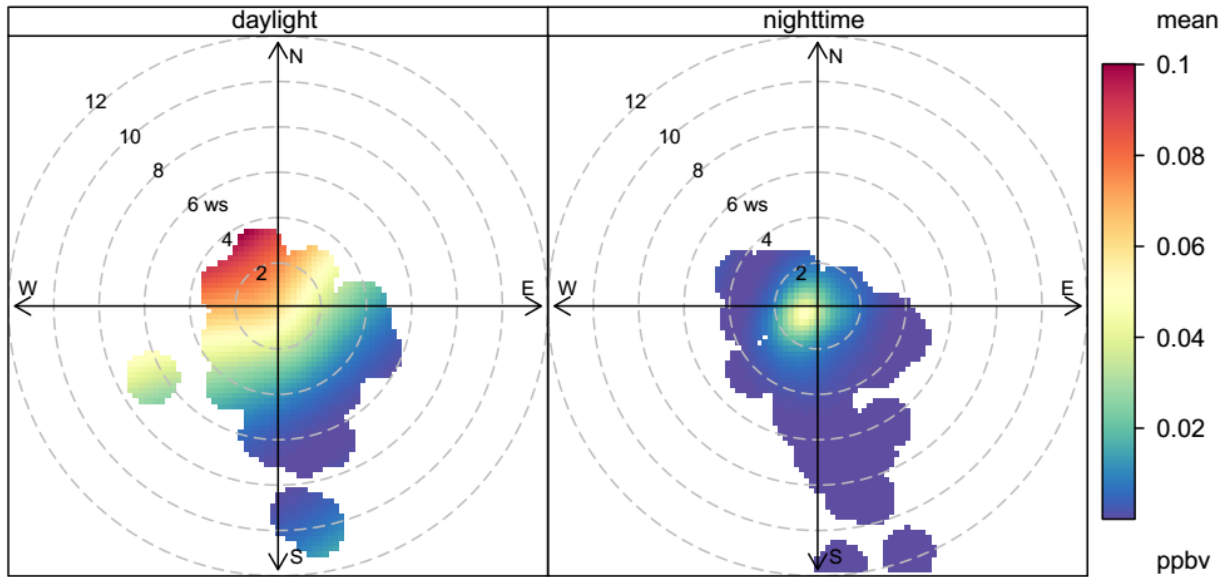


Figure 25: Polar plots of SO_2 as a function of wind direction and speed.

However, a more definitive indication of the source of SO_2 impacting NAA is the calculated hourly back trajectory data (Figure 26). As indicated in Figure 24, the highest concentration of SO_2 during the time when Factor 4 was present at NAA (by a factor of 5) occurred the evening of February 12. The back-trajectory plot associated with that peak is shown in Figure 26.

Footprint from HRRR-STILT model at NAA receptor (black triangle):
 2016-02-13 06:00 UTC -112.015 LON 40.711 LAT 10 m-AGL

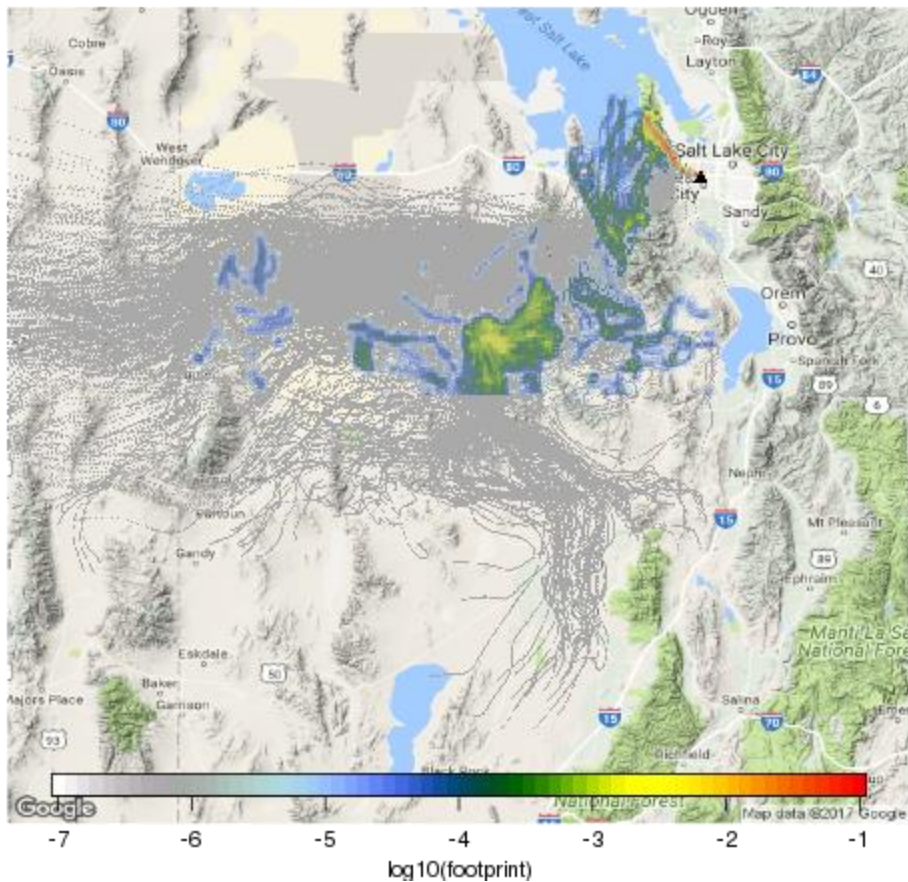


Figure 26: 24-hr back trajectory analysis of periods with enhanced SO₂.

Consistent with the polar plots, SO₂ present at NAA during this peak period originated from the NW with a very high probability. However, the back-trajectory changes direction at the boundary of the lake and came from the SW, clearly passing over the copper refinery. The probability of impact from the area of the oil refineries is near zero. Similar back-trajectories were observed through the 11-15 February 2016 cold pool period when Factor 4 was present. We conclude Factor 4 is associated with fugitive emissions from the copper smelter.

Factor 5 is present an average of 13.7 µg/m³, and represents 67.7% of the total PM_{2.5}. The mass of the factor is well explained by the PMF results (ratio of components to mass of 0.93). It contains 19% of the NVOM, 56% of the SVOM, 5% of the BC, 87% of the ammonium nitrate and 55% of the ammonium sulfate. Factor 5 is assumed to be associated with the secondary production of ammonium nitrate via reversible reaction of gaseous nitric acid and ammonia (NH₃).

Table 5: Factor Profiles of the 5 Factors Identified in the PMF Analysis Giving the Percent of Each Species in the Factor Profile.

	Factor 1	Factor 2	Factor 3	Factor 4	Factor 5
Species	Auto	Diesel	Wood Smoke	Smelter	Sec. Nitrate
PM _{2.5}	12.2	2.8	3.5	13.7	67.7
NVOM	35.0	12.2	8.2	7.8	19.1
SVOM	16.8	3.5	14.0	9.4	56.3
EC	0.0	91.8	1.9	6.2	0.0
BC	0.2	84.1	1.9	7.9	4.6
UV	5.3	82.1	4.4	6.3	1.9
NH ₄ NO ₃	0.7	0.0	0.0	12.7	86.5
(NH ₄) ₂ SO ₄	0.0	0.0	0.0	45.1	54.8
Chloride	2.3	18.8	0.2	14.5	64.2
Sodium	17.3	64.4	6.6	8.5	3.1
CO	73.2	0.0	0.0	8.6	18.1
NO _x	45.7	41.1	0.6	6.7	5.9
NO ₂	50.0	23.3	2.7	7.7	16.4
Fluorene	0.0	0.0	54.1	45.9	0.0
Levoglucosan	1.9	1.4	96.7	0.0	0.0
Stearic Acid	1.5	0.1	97.5	0.2	0.6
DHA Acid	42.8	0.4	56.5	0.1	0.2
Syringe Ald.	0.7	0.0	69.4	29.8	0.0
o-Phathalic A	0.0	0.0	0.1	98.4	1.5
Adipic Acid	0.0	0.0	6.1	93.8	0.0
4-oxyHD A.	0.1	0.3	86.2	0.1	13.3
Methanol	85.7	4.7	0.6	0.0	0.1
C8 Aromatics	70.5	12.5	9.6	2.0	8.6

Figure 27 gives the average concentration of each factor. The off-set factors (Auto, Diesel, Wood and Smelter) are related to primary emissions from the indicated sources. These factors combined account for 33% of the fine particulate material. The primary fine particulate material is dominated by the Smelter related factor and the Auto Related factor (14% and 12% of the total fine particulate material, respectively). The secondary fine particulate material is represented by the Nitrate related factor, which is 67% of the total.

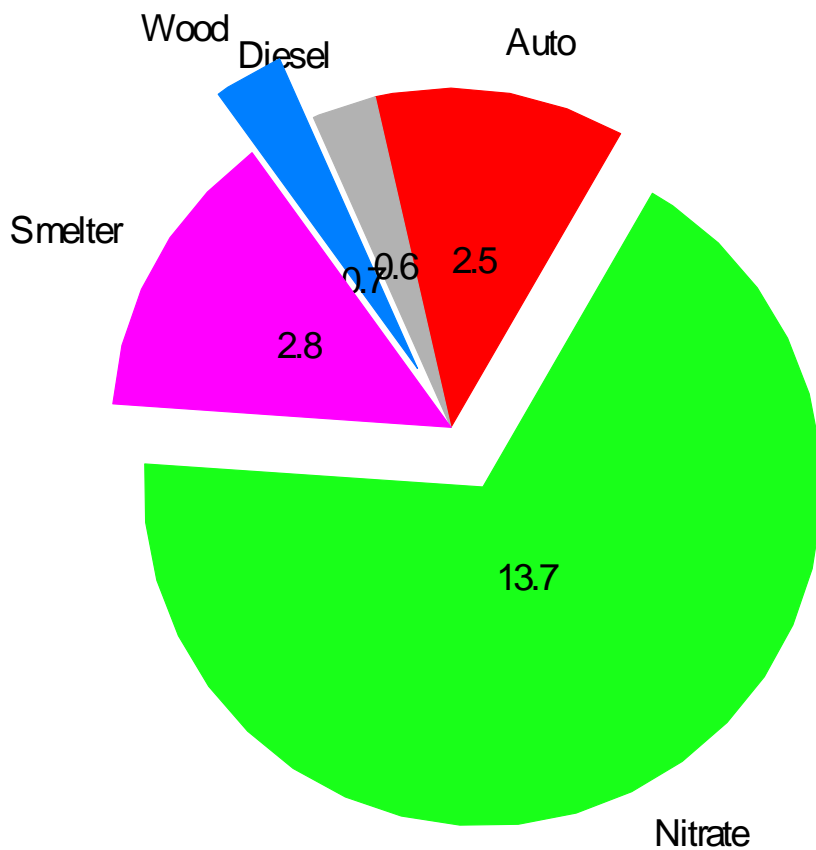
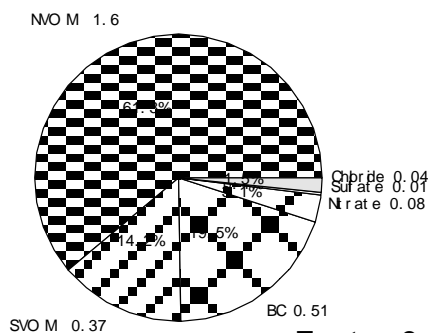


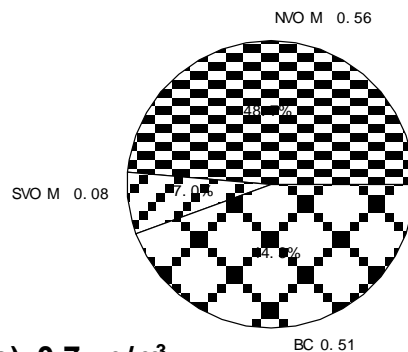
Figure 27: Pie chart of the final PMF factor results giving the average concentration of each factor. The average total $\text{PM}_{2.5}$ concentration is $20.3 \mu\text{g}/\text{m}^3$.

Both the primary Smelter related factor and the Secondary Nitrate related factor are present mainly during February 6-15, the time period of the persistent stagnation with the major cold pool seen during the study. The presence of the Smelter related factor during this time period can be attributed to the nature of the meteorological back trajectories during this time period and the presence of the secondary Nitrate related factor can be attributed to atmospheric chemistry leading to the formation of secondary components, dominated by ammonium nitrate and secondary NVOM and SVOM (Figure 22). It is worth noting that the primary Smelter related factor is present during the later stage of the PCAP, which coincides with fog events and period with plateauing $\text{PM}_{2.5}$.¹

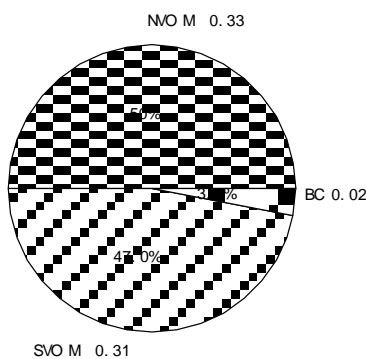
Factor 1 (Auto), 2.5 $\mu\text{g}/\text{m}^3$



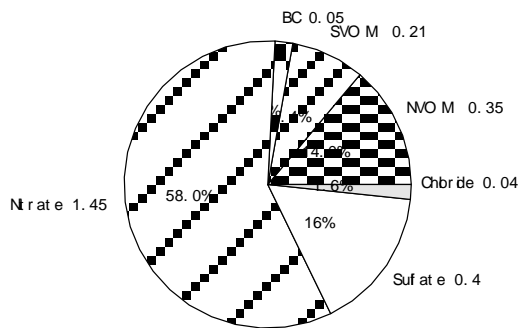
Factor 2 (Diesel), 0.6 $\mu\text{g}/\text{m}^3$



Factor 3 (Wood S m oke), 0.7 $\mu\text{g}/\text{m}^3$



Factor 4 (S m elter), 2.8 $\mu\text{g}/\text{m}^3$



Factor 5 (S ec. Nitr ate), 13.7 $\mu\text{g}/\text{m}^3$

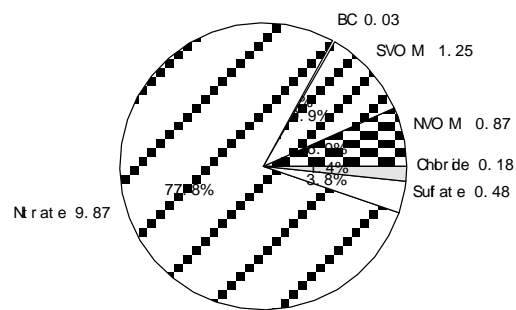


Figure 28: Pie charts giving the composition of each of the identified 5 factors in the PMF analysis.

As indicated in Figure 28, the composition of the primary factors Auto, Diesel and Wood Smoke were all dominated by carbonaceous material. In contrast, the Smelter related Factor 4 was dominated by ammonium sulfate and ammonium nitrate (74 % of the fine particulate mass), probable secondary material formed during transport from the smelter to NAA with 22% being carbonaceous in nature.

5.2.3. Back-trajectory analysis

Back-trajectory analysis was performed using the Stochastic Time-Inverted Lagrangian Transport (STILT) model to investigate the footprint and 24-hr back trajectory associated with the high formaldehyde and acetaldehyde events. STILT is a Lagrangian particle dispersion model that simulates atmospheric

transport with ensembles of stochastic air parcels represented by computational particles. The hourly data with CH₃CHO levels exceeding 5 ppb were selected and associated footprints (total of ~64 profiles) were examined. Figures 29 – 31 show representative footprints associated with the aldehyde events that took place between 12/24/2015 13:00 - 18:00, 01/05/2016 20:00 - 01/06/2016 12:00 and 01/30/2016 22:00 – 01/31/2016 8:00 MST. The footprints show a consistent pattern with a clearly defined, narrow trajectory within the Salt Lake Valley associated with wind directions between 150 – 200° and wider footprints in Utah Valley. UDAQ’s 2015 special air toxics study also found high levels of formaldehyde and acetaldehyde at the Bountiful site and attributed it to the sources in that area (Bountiful and North Salt Lake City area) including the local refineries, painting or paint stripping operations, and others. The West Valley Air Toxics Study also saw elevated levels of formaldehyde and acetaldehyde in West Valley City. Their diel variability in summer, with a small daytime peak, indicates that primary anthropogenic sources dominate the sources of these HAPs. Further analysis of wind pattern and back-trajectory analysis provide a footprint of the source region located south of NAA. This finding suggests that a wide variety of OVOC point sources are distributed across the Salt Lake Valley, including those sources in the North Salt Lake City and Bountiful area as suggested by Kuprov¹¹ and those in the southern part of the SLV based on back-trajectory analysis shown here. Given their importance as the ambient HAPs, more stringent controls of OVOCs are needed.

**Footprint from HRRR-STILT model at NAA receptor (black triangle):
2015-12-24 20:00 UTC -112.015 LON 40.711 LAT 10 m-AGL**

**Footprint from HRRR-STILT model at NAA receptor (black triangle):
2015-12-25 02:00 UTC -112.015 LON 40.711 LAT 10 m-AGL**

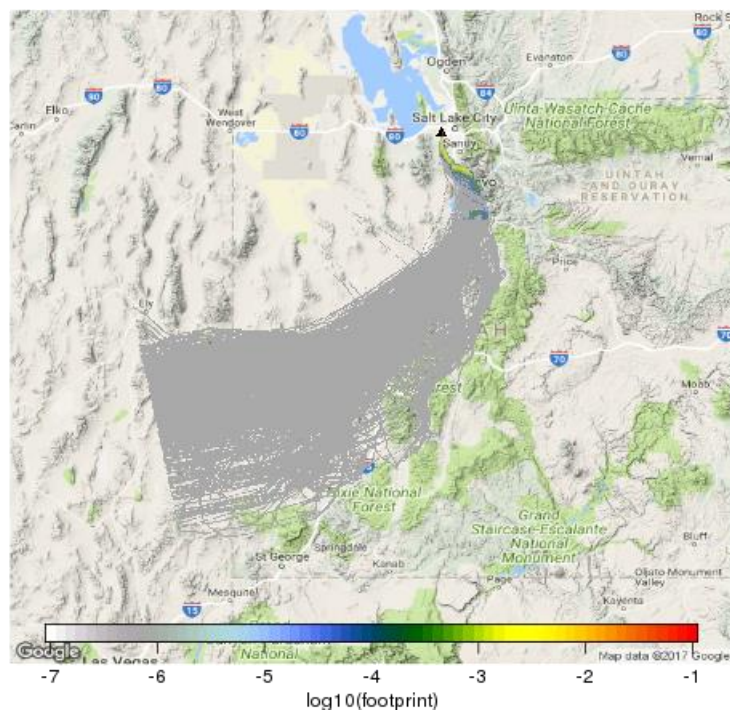
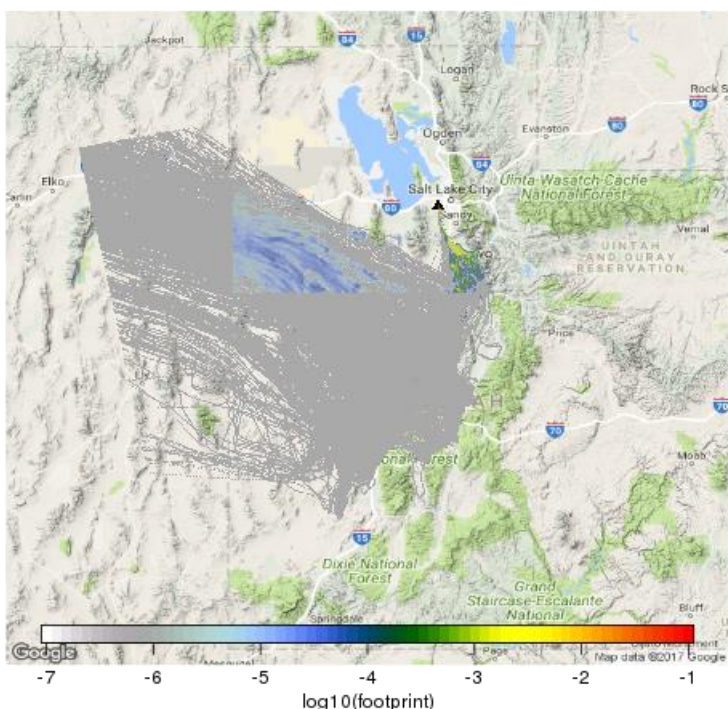
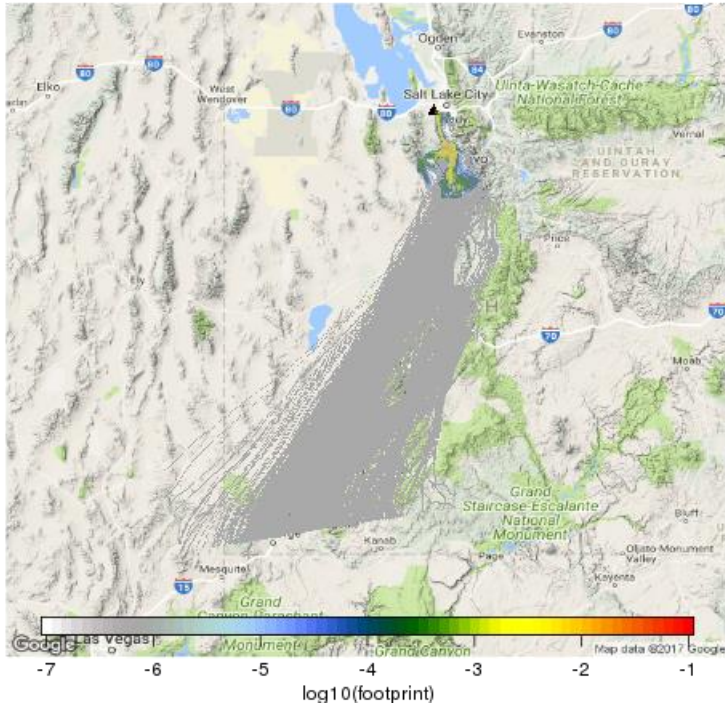
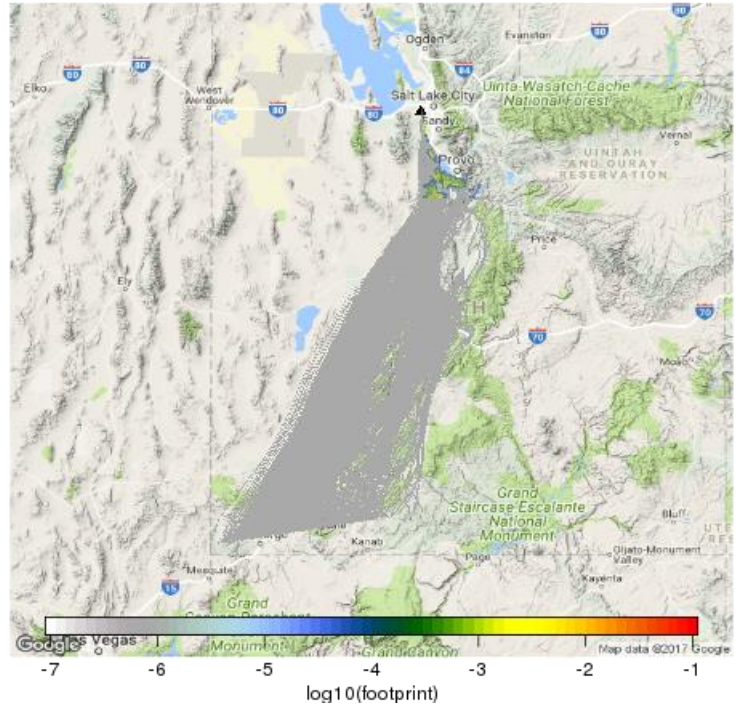


Figure 29: 24-hr back trajectory associated with high aldehyde event that occurred between 12/24/2015 13:00 - 18:00 MS

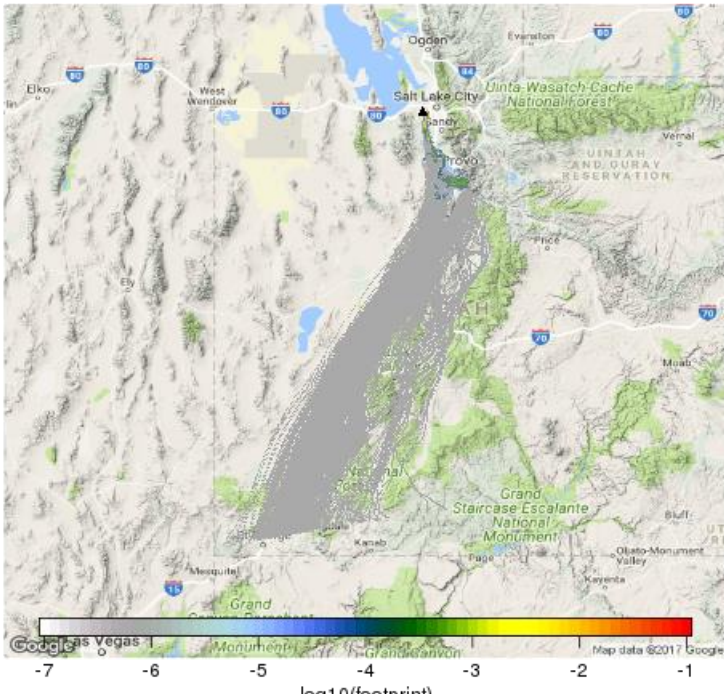
**Footprint from HRRR-STILT model at NAA receptor (black triangle):
2016-01-06 09:00 UTC -112.015 LON 40.711 LAT 10 m-AGL**



**Footprint from HRRR-STILT model at NAA receptor (black triangle):
2016-01-06 10:00 UTC -112.015 LON 40.711 LAT 10 m-AGL**



**Footprint from HRRR-STILT model at NAA receptor (black triangle):
2016-01-06 15:00 UTC -112.015 LON 40.711 LAT 10 m-AGL**



**Footprint from HRRR-STILT model at NAA receptor (black triangle):
2016-01-06 20:00 UTC -112.015 LON 40.711 LAT 10 m-AGL**

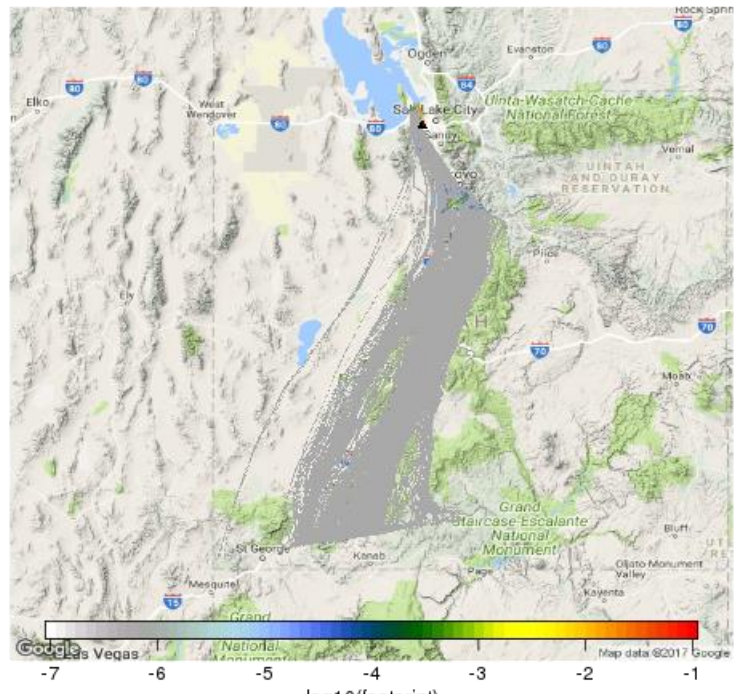
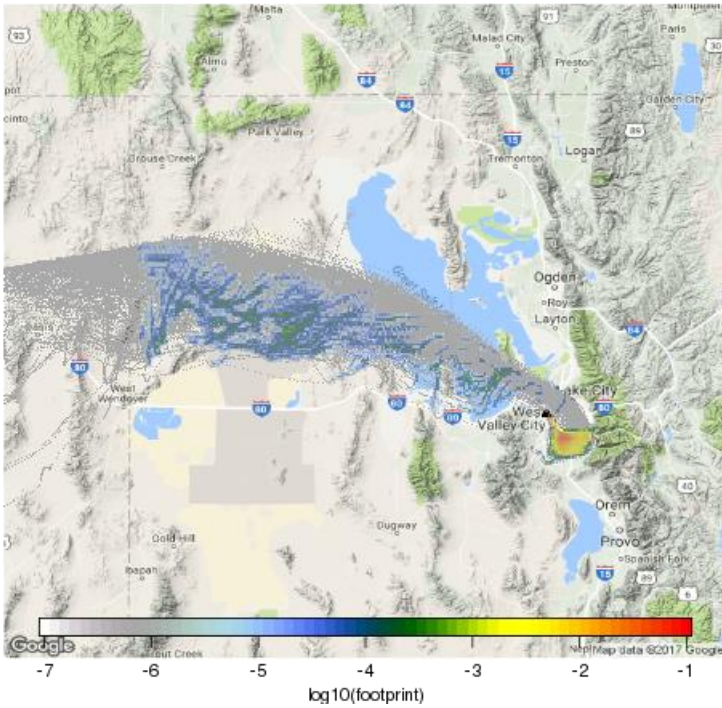
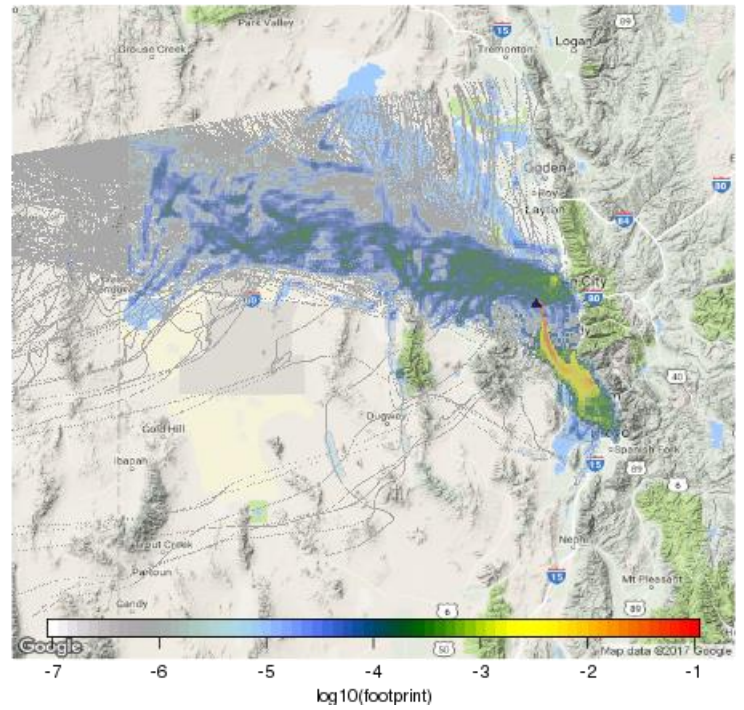


Figure 30: 24-hr back trajectory associated with high aldehyde event that occurred between 01/05/2016 20:00 – 01/06/2016 12:00 MST. The last panel shows footprint for 01/06/2016 13:00 MST associated with northerly winds from the lake that brought the levels of aldehydes down by half.

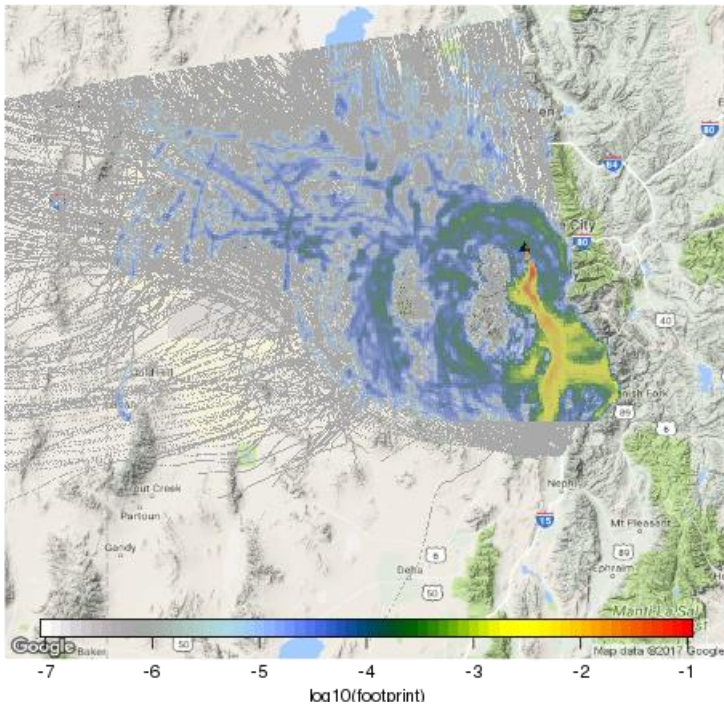
**Footprint from HRRR-STILT model at NAA receptor (black triangle):
2016-01-31 06:00 UTC -112.015 LON 40.711 LAT 10 m-AGL**



**Footprint from HRRR-STILT model at NAA receptor (black triangle):
2016-01-31 08:00 UTC -112.015 LON 40.711 LAT 10 m-AGL**



**Footprint from HRRR-STILT model at NAA receptor (black triangle):
2016-01-31 12:00 UTC -112.015 LON 40.711 LAT 10 m-AGL**



**Footprint from HRRR-STILT model at NAA receptor (black triangle):
2016-01-31 19:00 UTC -112.015 LON 40.711 LAT 10 m-AGL**

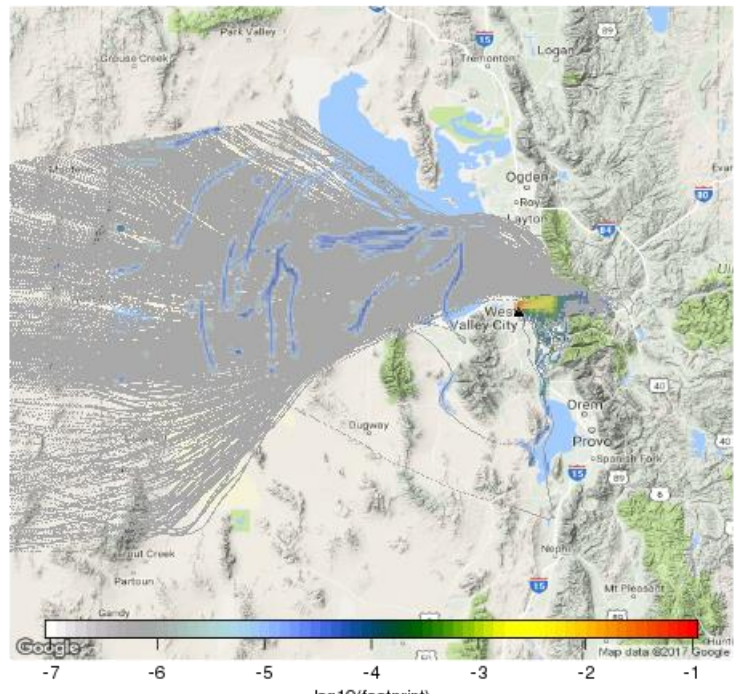


Figure 31: 24-hr back trajectory associated with high aldehyde event that occurred between 01/30/2016 22:00 – 01/31/16 10: 00 MST. The last panel shows footprint for 01/06/2016 12:00 MST associated with easterly winds and lower levels of aldehydes.

6. Implications for Air Quality

West Valley City Air Toxics Monitoring Campaign was also critical to further the understanding of the $PM_{2.5}$ pollution episodes as it provided a wide array of real time measurements of trace gas and particulate matter at a central location in the SLV valley. A comparison of the observations at NAA with

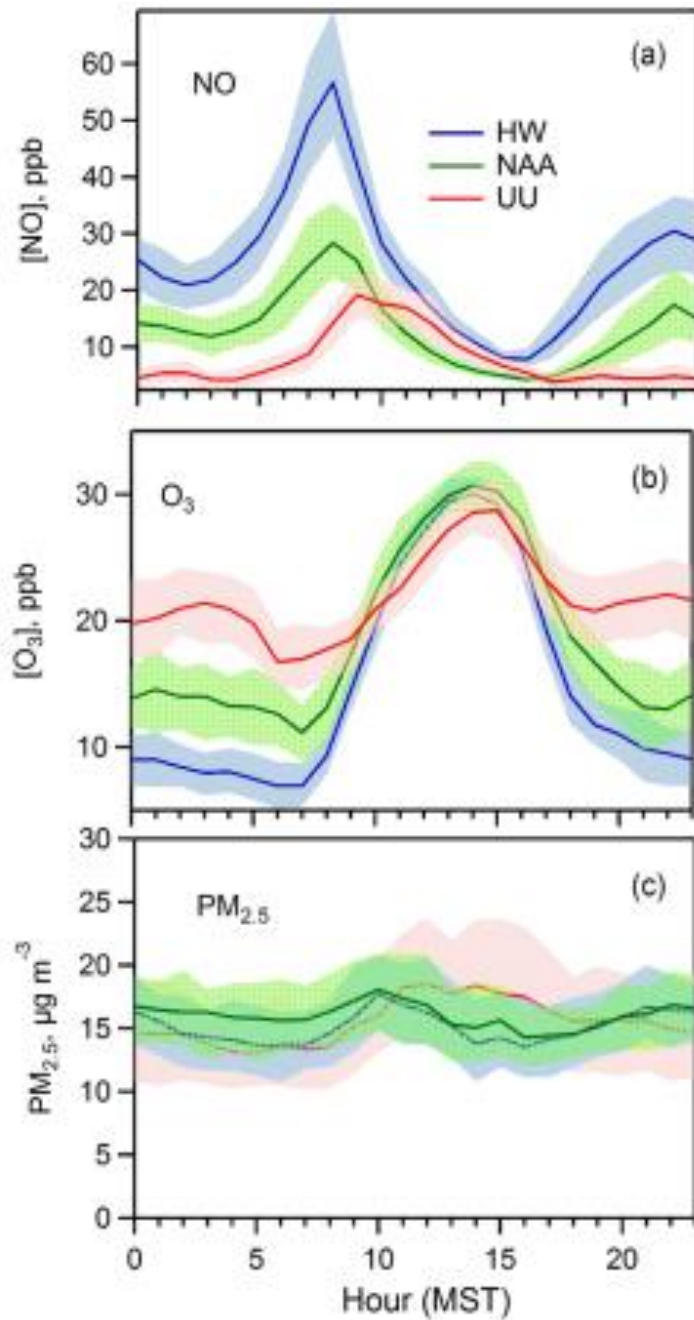


Figure 32: Diurnal variation of (a) NO and (b) O₃ mixing ratios and (c) PM_{2.5} mass concentrations at HW, NAA, and UU sites during 2015-2016 winter¹.

those at HW and UU show a considerable variation from site to site with lowest NO_x and highest O_3 observed at the UU site located on the eastern bench of the Wasatch Front. In contrast, $\text{PM}_{2.5}$ levels are relatively homogeneous across the valley¹ (Figure 32). This comparison shed light on the chemical mechanism for secondary $\text{PM}_{2.5}$ formation and build up, which appears to be dominated by nighttime aerosol nitrate formation in the upper part of a PCAP and a subsequent mixing during the day to distribute the pollutants vertically within the PCAP and horizontally across the valley¹. This work led to a large-scale aircraft study called Utah Winter Fine Particulate Study (UWFPS), which took place 2016-2017 winter.

<https://www.esrl.noaa.gov/csd/groups/csd7/measurements/2017uwfps/>

The aerosol composition data and PMF analysis at NAA confirm the importance of the secondary NH_4NO_3 during the wintertime pollution episodes in the SLV. Although NH_4NO_3 formation appears to be nitrate-limited based on the wintertime observations of gaseous and particulate reduced and oxidized nitrogen species at NAA, the system is less nitrate limited during the wintertime pollution episodes, suggesting potential significance of NH_3 .

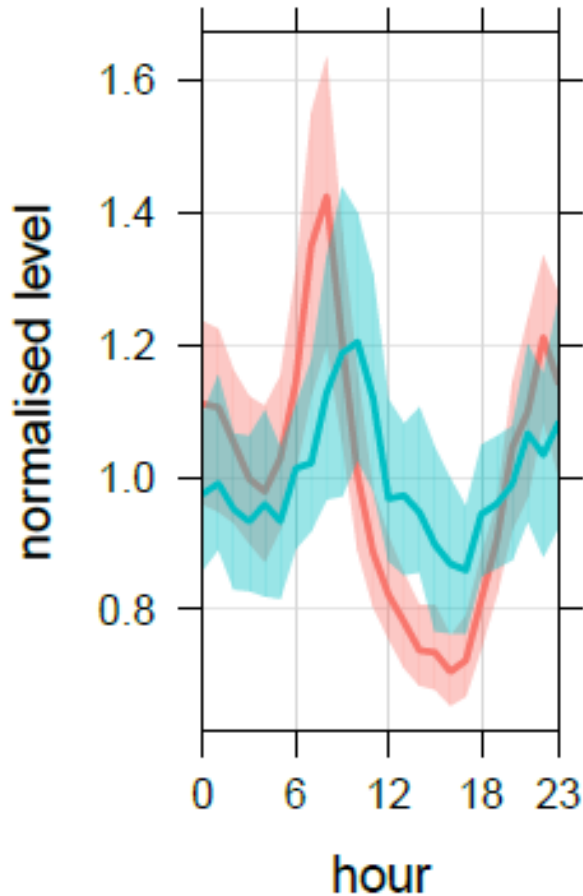


Figure 33: Diurnal variations of NH₃ (teal) and benzene (pink) at NAA during 2015-2016 winter to indicate the hour lag of NH₃ peak.

Figure 33 shows their diel profiles of NH₃ and benzene at NAA. NH₃ levels peak during the day at ~ 11 AM as shown in Figure 33. In contrast, the benzene, CO and NO_x from mobile sources show enhancements at ~ 10 AM during the winter, suggesting the presence of NH₃ sources other mobile sources in the SLV.

Further analysis of the wind direction and speed, and the back trajectory analysis suggest that the elevated levels of NH₃ (and NH_x) at NAA are associated with the southerly flows. Figure 34 presents an example case 01/13/2016 to highlight the importance of the nighttime inter-basin transport and drainage flows from Utah Valley to SLV as indicated by Mesowest surface wind measurements¹².

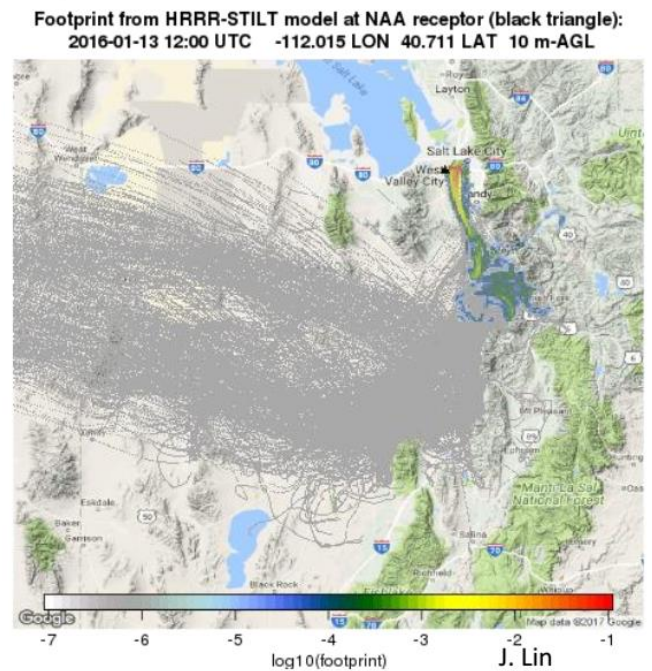
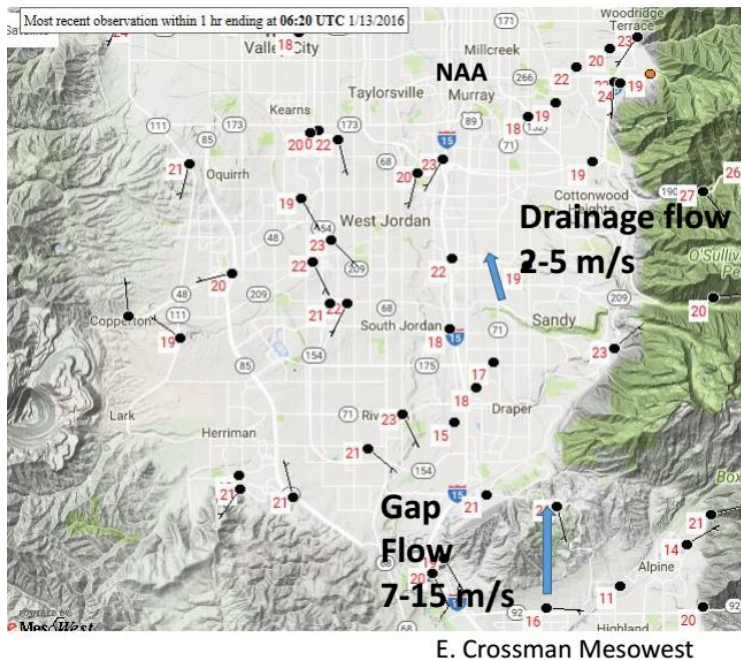


Figure 34: A case study (January 13, 2016) illustrating the inter-valley exchange processes that can transport of NH_3 and other pollutants from down south, potentially from Utah Valley to the SLV.

The STILT 24-hr back trajectory analysis predicts a consistent footprint that indicates a transport from down south. Depending on the wind speed, the transport time from the Jordan Narrows (southern gap) to NAA would be 3 - 7 hours and can lead to enhancement in NH_3 during the day. Consistently, a daytime NH_3 peak was observed at ~ 11 AM on January 13, 2016. Surface measurements at NAA, STILT back trajectory analysis, and surface wind data all support nighttime transport of NH_3 from the south, likely from Utah Valley to SLV. A detailed analysis of equilibrium conditions, limiting reagents and NH_3 sources is required to fully characterize the processes important for the $\text{PM}_{2.5}$ formation and is beyond the scope of this report. Nonetheless, our observations show that NAA is possibly more representative site to study valley wide emission and/or pollution distribution due to its central location on the path of various exchange processes, and an ideal place for future air quality or toxics studies.

7. Public Outreach

Our monitoring campaign was based at Neil Armstrong Academy, an elementary school dedicated to science, technology, and math. This collaboration offered us unique outreach and educational opportunities to reach out to the students and the community. We organized a media event at NAA during our winter campaign. As part of the media event, all of the 5-6th grade classes were invited to participate in an air quality lecture and question and answer session.

<http://fox13now.com/2016/01/26/study-underway-to-understand-how-to-make-utah-air-cleaner-safer-to-breathe/>

As part of the outreach activity, we made news releases to reach out to public, hosted an open house in our measurement site and made presentations to discuss health impacts of HAPs, air quality and preliminary results. We also made demonstrations to show how the emissions from various sources get trapped in the valley, how they affect our health, and how individuals can help to protect and help reduce pollution.

8. Summary

As part of West Valley High Time Resolution Air Toxics Monitoring campaign, a wide array of gaseous and particulate HAPs and related species were monitored at Neil Armstrong Academy located in the West Valley City to provide real-time observations of trace gas and particulate composition during summer and winter season. The study generated a rich dataset of HAPs, including speciated organics in both gas and particulate phase. The ambient levels, temporal trends and wind pattern variability, and source signatures of the monitored HAPs were examined to deduce information on their predominant sources. High time resolution observations of VOCs indicate high levels of OVOCs including small aldehydes and carbonyl compounds (e.g.) in the SLV. The comprehensive analysis suggests a wide variety of anthropogenic OVOC sources contribute to the observed levels and more stringent regulations on the OVOC sources (that may include solvent usage, paint stripping etc.) are needed. Consistent with the UDAQ's 2015 special air toxics study, this work also saw elevated levels of form- and acetaldehyde in West Valley City. Their diel variability in summer with a small daytime peak indicate that primary anthropogenic sources dominate the sources of these HAPs. Further analysis of wind pattern and back-trajectory analysis provide a footprint of the source region located south of NAA, lending evidence of a wide variety of OVOC sources within the SLV. Given their importance as ambient HAPs, more stringent controls of OVOCs are needed.

A Positive Matrix Factorization (PMF) analysis was conducted to identify probable sources of the fine particulate material. Input to the analysis included the FDMS TEOM measured fine particulate mass, the components of the PM_{2.5}, gas phase species which contribute the identification of sources and secondary chemistry (CO, NO_x and NO₂) and specific markers of primary and secondary contributors to PM_{2.5} (Fluorene, Levoglucosan, Dehydroabietic Acid, Syringe Aldehyde, o-Phthalic Acid, Adipic Acid, 4-oxyheptanedioic Acid, Methanol and C₈ Aromatics). A total of 689 hourly averaged data sets were available for this analysis.

Five factors were identified in this analysis. They were characterized as being associated with primary emissions of secondary aerosol formation based on the composition of the factor profile and the diurnal pattern of the factor concentrations. Two of the factors were associated with emissions from auto and diesel vehicles. One was associated with emission from the wood combustion. One was associated with fugitive emissions from the copper smelter to the west of NAA (the identification of the source of this factor was greatly aided using back-trajectory information). Factor 5 was associated with the formation of secondary aerosol, dominated by ammonium nitrate.

Based on this analysis, PM_{2.5} was 33% primary and 67% secondary during the time of the data for the analysis was done. The major contributors to the primary fine particulate material were the fugitive emissions from the copper smelter and automobile emissions.

A rich dataset collected as part of this campaign was also used for a comprehensive analysis to improve scientific understanding of the fundamental chemical and meteorological processes underlying $PM_{2.5}$ formation in the SLV in winter as discussed in Baasandorj et al. ¹ and motivated in-depth research to improve the air quality.

9. References

1. Baasandorj, M.; Hoch, S. W.; Bares, R.; Lin, J. C.; Brown, S. S.; Millet, D. B.; Martin, R.; Kelly, K.; Zarzana, K. J.; Whiteman, C. D.; Dube, W. P.; Tonnesen, G.; Jaramillo, I. C.; Sohl, J., Coupling between Chemical and Meteorological Processes under Persistent Cold-Air Pool Conditions: Evolution of Wintertime PM_{2.5} Pollution Events and N₂O₅ Observations in Utah's Salt Lake Valley. *Environ Sci Technol* **2017**, DOI 10.1021/acs.est.6b06603.
2. *A Snapshot of 2050: An Analysis of Population Change in Utah*; Utah Foundation: Salt Lake City, UT, 2014; <http://www.utahfoundation.org/uploads/rr720.pdf> (Last accessed: 11/2017).
3. Kelly, K. E.; Kotchenruther, R.; Kuprov, R.; Silcox, G. D., Receptor model source attributions for Utah's Salt Lake City airshed and the impacts of wintertime secondary ammonium nitrate and ammonium chloride aerosol. *Journal of the Air & Waste Management Association* **2013**, *63* (5), 575-590. DOI 10.1080/10962247.2013.774819.
4. Silcox, G. D.; Kelly, K. E.; Crosman, E. T.; Whiteman, C. D.; Allen, B. L., Wintertime PM_{2.5} concentrations during persistent, multi-day cold-air pools in a mountain valley. *Atmos. Environ.* **2012**, *46*, 17-24. DOI 10.1016/j.atmosenv.2011.10.041.
5. Whiteman, C. D.; Hoch, S. W.; Horel, J. D.; Charland, A., Relationship between particulate air pollution and meteorological variables in Utah's Salt Lake Valley. *Atmos. Environ.* **2014**, *94*, 742-753. DOI 10.1016/j.atmosenv.2014.06.012.
6. Lareau, N. P.; Crosman, E.; Whiteman, C. D.; Horel, J. D.; Hoch, S. W.; Brown, W. O. J.; Horst, T. W., The Persistent Cold-Air Pool Study. *Bull. Am. Meteorol. Soc.* **2013**, *94* (1), 51. DOI 0.1175/BAMS-D-11-00255.1.
7. Beard, J. D.; Beck, C.; Graham, R.; Packham, S. C.; Traphagan, M.; Giles, R. T.; Morgan, J. G., Winter temperature inversions and emergency department visits for asthma in Salt Lake County, Utah, 2003-2008. *Environ. Health Perspect.* **2012**, *120* (10), 1385. DOI 10.1289/ehp.1104349.
8. *2012 Utah Ozone Study*; Utah Division of Air Quality: 2013; https://deq.utah.gov/Pollutants/O/ozone/docs/2013/05May/2012_Utah_Ozone_Study.pdf (Last accessed: 11/2017).
9. Blaylock, B. K.; Horel, J. D.; Crosman, E. T., Impact of lake breezes on summer ozone concentrations in the salt lake valley.(Author abstract). *Journal of Applied Meteorology and Climatology* **2017**, *56* (2), 353. DOI 10.1175/JAMC-D-16-0216.1.
10. *Hazardous Air Pollutants*; United States Environmental Protection Agency: 2016; <https://www.epa.gov/haps> (Last accessed: November 9, 2017).
11. *2015 Special Toxics Study Report*; 2016; <https://deq.utah.gov/Pollutants/H/haps/docs/2015-Special-Toxics-Study.pdf>.
12. Horel, J.; Splitt, M.; Dunn, L.; Pechmann, J.; White, B.; Ciliberti, C.; Lazarus, S.; Slemmer, J.; Zaff, D.; Burks, J., Mesowest: cooperative Mesonets in the western United States.(Abstract). *Bulletin of the American Meteorological Society* **2002**, *83* (2), 165. DOI 10.1175/1520-0477(2002)083<0879:EDOTCU>2.3.CO2.
13. Kuprov, R.; Eatough, D. J.; Cruickshank, T.; Olson, N.; Cropper, P. M.; Hansen, J. C., Composition and secondary formation of fine particulate matter in the Salt Lake Valley: Winter 2009. *J. Air Waste Manage. Assoc.* **2014**, *64* (8), 957-969. DOI 10.1080/10962247.2014.903878.
14. Cropper, P. M.; Eatough, D. J.; Overson, D. K.; Hansen, J. C.; Caka, F.; Cary, R. A., Use of a GC-MS Organic Aerosol Monitor for In-Field Detection of Fine Particulate Organic Compounds in Source Apportionment. *Journal of the Air & Waste Management Association* **2017**, null-null. DOI 10.1080/10962247.2017.1363095.

15. Cropper, P. M.; Overson, D. K.; Cary, R. A.; Eatough, D. J.; Chow, J. C.; Hansen, J. C., Development of the GC-MS organic aerosol monitor (GC-MS OAM) for in-field detection of particulate organic compounds. *Atmospheric Environment* **2017**, *169*, 258-266. DOI 10.1016/j.atmosenv.2017.09.019.
16. Baasandorj, M.; Millet, D. B.; Hu, L.; Mitroo, D.; Williams, B. J., Measuring acetic and formic acid by proton-transfer-reaction mass spectrometry: sensitivity, humidity dependence, and quantifying interferences. *Atmos. Meas. Tech.* **2015**, *8* (3), 1303-1321. DOI 10.5194/amt-8-1303-2015.
17. Hu, L.; Millet, D. B.; Baasandorj, M.; Griffis, T. J.; Turner, P.; Helmig, D.; Curtis, A. J.; Hueber, J., Isoprene emissions and impacts over an ecological transition region in the U.S. Upper Midwest inferred from tall tower measurements. *Journal of Geophysical Research: Atmospheres* **2015**, *120* (8), 3553-3571. DOI 10.1002/2014JD022732.
18. Hu, L.; Millet, D. B.; Kim, S. Y.; Wells, K. C.; Griffis, T. J.; Fischer, E. V.; Helmig, D.; Hueber, J.; Curtis, A. J., North American acetone sources determined from tall tower measurements and inverse modeling. *Atmos. Chem. Phys.* **2013**, *13* (6), 3379-3392. DOI 10.5194/acp-13-3379-2013.
19. de Gouw, J.; Warneke, C., Measurements of volatile organic compounds in the earth's atmosphere using proton-transfer-reaction mass spectrometry. *Mass Spectrom. Rev.* **2007**, *26* (2), 223-257. DOI 10.1002/mas.20119.
20. Warneke, C.; van Der Veen, C.; Luxembourg, S.; de Gouw, J. A.; Kok, A., Measurements of benzene and toluene in ambient air using proton-transfer-reaction mass spectrometry: calibration, humidity dependence, and field intercomparison. *International Journal of Mass Spectrometry* **2001**, *207* (3), 167-182. DOI 10.1016/S1387-3806(01)00366-9.
21. de Gouw, J. A.; Goldan, P. D.; Warneke, C.; Kuster, W. C.; Roberts, J. M.; Marchewka, M.; Bertman, S. B.; Pszenny, A. A. P.; Keene, W. C., Validation of proton transfer reaction-mass spectrometry (PTR-MS) measurements of gas-phase organic compounds in the atmosphere during the New England Air Quality Study (NEAQS) in 2002. *Journal of Geophysical Research: Atmospheres* **2003**, *108* (D21), n/a-n/a. DOI 10.1029/2003JD003863.
22. Hu, L.; Millet, D. B.; Baasandorj, M.; Griffis, T. J.; Travis, K. R.; Tessum, C. W.; Marshall, J. D.; Reinhart, W. F.; Mikoviny, T.; Müller, M.; Wisthaler, A.; Graus, M.; Warneke, C.; Gouw, J., Emissions of C6–C8 aromatic compounds in the United States: Constraints from tall tower and aircraft measurements. *J. Geophys. Res.: Atmos.* **2015**, *120* (2), 826-842. DOI 10.1002/2014JD022627.
23. Paatero, P., Least squares formulation of robust non-negative factor analysis. *Chemometrics and Intelligent Laboratory Systems* **1997**, *37* (1), 23-35. DOI [https://doi.org/10.1016/S0169-7439\(96\)00044-5](https://doi.org/10.1016/S0169-7439(96)00044-5).
24. Grover, B. D.; Eatough, D. J., Source Apportionment of One-Hour Semi-Continuous Data Using Positive Matrix Factorization with Total Mass (Nonvolatile plus Semi-Volatile) Measured by the R&P FDMS Monitor. *Aerosol Science and Technology* **2008**, *42* (1), 28-39. DOI 10.1080/02786820701787910.
25. Polissar, A. V.; Hopke, P. K.; Paatero, P.; Malm, W. C.; Sisler, J. F., Atmospheric aerosol over Alaska: 2. Elemental composition and sources. *Journal of Geophysical Research: Atmospheres* **1998**, *103* (D15), 19045-19057. DOI 10.1029/98JD01212.
26. Lin, J. C.; Gerbig, C.; Wofsy, S. C.; Andrews, A. E.; Daube, B. C.; Davis, K. J.; Grainger, C. A., A near-field tool for simulating the upstream influence of atmospheric observations: The Stochastic Time-Inverted Lagrangian Transport (STILT) model. *Journal of Geophysical Research: Atmospheres* **2003**, *108* (D16), n/a-n/a. DOI 10.1029/2002JD003161.
27. Wen, D.; Lin, J. C.; Millet, D. B.; Stein, A. F.; Draxler, R. R., A backward-time stochastic Lagrangian air quality model. *Atmospheric Environment* **2012**, *54*, 373-386. DOI 10.1016/j.atmosenv.2012.02.042.
28. *Technical Assistance Document (TAD) For Precursor Gas Measurements in the NCore Multi-Pollutant Monitoring Network*; United States Environmental Protection Agency: 2005; <https://www3.epa.gov/ttnamti1/ncoreguidance.html> (Last accessed: May 9, 2017).

29. Veres, P.; Roberts, J. M.; Warneke, C.; Welsh-Bon, D.; Zahniser, M.; Herndon, S.; Fall, R.; de Gouw, J., Development of negative-ion proton-transfer chemical-ionization mass spectrometry (NI-PT-CIMS) for the measurement of gas-phase organic acids in the atmosphere. *International Journal of Mass Spectrometry* **2008**, 274 (1), 48-55. DOI 10.1016/j.ijms.2008.04.032.
30. Roberts, J. M.; Veres, P.; Warneke, C.; Neuman, J. A.; Washenfelder, R. A.; Brown, S. S.; Baasandorj, M.; Burkholder, J. B.; Burling, I. R.; Johnson, T. J.; Yokelson, R. J.; de Gouw, J., Measurement of HONO, HNCO, and other inorganic acids by negative-ion proton-transfer chemical-ionization mass spectrometry (NI-PT-CIMS): application to biomass burning emissions. *Atmos. Meas. Tech.* **2010**, 3 (4), 981-990. DOI 10.5194/amt-3-981-2010.